Enhanced Sampling Algorithms

3 AUTHORS:

Ayori Mitsutake
Keio University

33 PUBLICATIONS **1,020** CITATIONS

SEE PROFILE

Yoshiharu Mori
Institute for Molecular Science

16 PUBLICATIONS **81** CITATIONS

SEE PROFILE

Yuko Okamoto
Nagoya University

231 PUBLICATIONS **7,648** CITATIONS

SEE PROFILE

ENHANCED SAMPLING ALGORITHMS

Ayori Mitsutake,[a] Yoshiharu Mori,[b] and Yuko Okamoto[b,c,1]

[a]*Department of Physics*
Keio University
Yokohama, Kanagawa 223-8522, Japan
[b]*Department of Physics*
Nagoya University
Nagoya, Aichi 464-8602, Japan
[c]*Structural Biology Research Center*
Nagoya University
Nagoya, Aichi 464-8602, Japan

ABSTRACT

In biomolecular systems (especially all-atom models) with many degrees of freedom such as proteins and nucleic acids, there exist an astronomically large number of local-minimum-energy states. Conventional simulations in the canonical ensemble are of little use, because they tend to get trapped in states of these energy local minima. Enhanced conformational sampling techniques are thus in great demand. A simulation in generalized ensemble performs a random walk in potential energy space and can overcome this difficulty. From only one simulation run, one can obtain canonical-ensemble averages of physical quantities as functions of temperature by the single-histogram and/or multiple-histogram reweighting techniques. In this article we review uses of the generalized-ensemble algorithms in biomolecular systems. Three well-known methods, namely, multicanonical algorithm, simulated tempering, and replica-exchange method, are described first. Both Monte Carlo and molecular dynamics versions of the algorithms are given. We then present various extensions of these three generalized-ensemble algorithms. The effectiveness of the methods is tested with short peptide and protein systems.

[1] Corresponding author. e-mail: okamoto@phys.nagoya-u.ac.jp

1   INTRODUCTION

Conventional Monte Carlo (MC) and molecular dynamics (MD) simulations of biomolecules are greatly hampered by the multiple-minima problem. The canonical fixed-temperature simulations at low temperatures tend to get trapped in a few of a huge number of local-minimum-energy states which are separated by high energy barriers. One way to overcome this multiple-minima problem is to perform a simulated annealing (SA) simulation [1], and it has been widely used in biomolecular systems (see, e.g., Refs. [2]–[8] for earlier applications). The SA simulation mimicks the crystal-making process, and temperature is lowered very slowly from a sufficiently high temperature to a low one during the SA simulation. The Boltzmann weight factor is dynamically changed, and so the thermal equilibrium is continuously broken. Hence, although the global-minimum potential energy or the value close to it may be found, accurate thermodynamic averages for fixed temperatures cannot be obtained.

A class of simulation methods, which are referred to as the *generalized-ensemble algorithms*, overcome both above difficulties, namely the multipole-minima problem and inaccurate thermodynamic averages (for reviews see, e.g., Refs. [9]–[16]). In the generalized-ensemble algorithm, each state is weighted by an artificial, non-Boltzmann probability weight factor so that a random walk in potential energy space may be realized. The random walk allows the simulation to escape from any energy barrier and to sample much wider conformational space than by conventional methods. Unlike SA simulations, the weight factors are fixed during the simulations so that the eventual reach to the thermal equilibrium is guaranteed. From a single simulation run, one can obtain accurate ensemble averages as functions of temperature by the single-histogram [17] and/or multiple-histogram [18, 19] reweighting techniques (an extension of the multiple-histogram method is also referred to as the *weighted histogram analysis method* (WHAM) [19]).

One of the most well-known generalized-ensemble algorithms is perhaps the *multi-canonical algorithm* (MUCA) [20, 21] (for reviews see, e.g., Refs. [22, 23]). The method is also referred to as *entropic sampling* [24, 25] and *adaptive umbrella sampling* [26] *of the potential energy* [27]. MUCA can also be considered as a sophisticated, ideal realization of a class of algorithms called *umbrella sampling* [28]. Also closely related methods are *Wang-Landau method* [29, 30], which is also referred to as *density of states Monte Carlo* [31], and *Meta Dynamics* [32]. See also Ref. [33]. MUCA and its generalizations have been applied to spin systems (see, e.g., Refs. [34]–[40]). MUCA was also introduced to the molecular simulation field [41]. Since then MUCA and its generalizations have been extensively used in many applications in protein and other biomolecular systems [42]–[76]. Molecular dynamics version of MUCA has also been developed [48, 52, 27] (see also Refs. [77, 48] for the Langevin dynamics version). MUCA has been extended so that flat distributions in other variables instead of potential energy may be obtained (see, e.g., Refs. [35, 36, 47, 53, 55, 68, 74]). This can be considered as a special case of the multidimensional (or, multivariable) extensions of MUCA, where a multidimensional random walk in potential energy space and in other variable space is realized (see, e.g., Refs. [47, 53, 54, 70, 76]). In this article, we just present one of such methods, namely, the *multibaric-multithermal algorithm* (MUBATH) where a two-dimensional random walk in both potential energy space and volume space is realized [70]–[73].

While a simulation in multicanonical ensemble performs a free 1D random walk in potential energy space, that in *simulated tempering* (ST) [78, 79] (the method is also

referred to as the *method of expanded ensemble* [78]) performs a free random walk in temperature space (for a review, see, e.g., Ref. [80]). This random walk, in turn, induces a random walk in potential energy space and allows the simulation to escape from states of energy local minima. ST and its generalizations have also been applied to chemical physics field and biomolecular systems [81, 82, 49, 50, 83, 84, 85, 86, 87, 88, 89].

MUCA and ST are powerful, but the probability weight factors are not *a priori* known and have to be determined by iterations of short trial simulations. This process can be non-trivial and very tedius for complex systems with many degreees of freedom.

In the *replica-exchange method* (REM) [90]–[92], the difficulty of weight factor determination is greatly alleviated. (A closely related method was independently developed in Ref. [93]. Similar methods in which the same equations are used but emphasis is laid on optimizations have been developed [94, 95]. REM is also referred to as *multiple Markov chain method* [96] and *parallel tempering* [80]. Details of literature about REM and related algorithms can be found in recent reviews [97, 10, 15].) In this method, a number of non-interacting copies (or, replicas) of the original system at different temperatures are simulated independently and simultaneously by the conventional MC or MD method. Every few steps, pairs of replicas are exchanged with a specified transition probability. The weight factor is just the product of Boltzmann factors, and so it is essentially known.

REM has already been used in many applications in protein systems [98]–[113]. Other molecular simulation fields have also been studied by this method in various ensembles [114]–[118]. Moreover, REM was introduced to the quantum chemistry field [119]. The details of molecular dynamics algorithm for REM, which is referred to as the *Replica-Exchange Molecular Dynamics* (REMD) have been worked out in Ref. [99], and this led to a wide application of REM in the protein folding and related problems (see, e.g., Refs. [120]–[142]).

However, REM also has a computational difficulty: As the number of degrees of freedom of the system increases, the required number of replicas also greatly increases, whereas only a single replica is simulated in MUCA and ST. This demands a lot of computer power for complex systems. Our solution to this problem is: Use REM for the weight factor determinations of MUCA, which is much simpler than previous iterative methods of weight determinations, and then perform a long MUCA production run. The method is referred to as the *replica-exchange multicanonical algorithm* (REMUCA) [103, 107, 108]. In REMUCA, a short replica-exchange simulation is performed, and the multicanonical weight factor is determined by the multiple-histogram reweighting techniques [18, 19]. Another example of a combination of REM and ST is the *replica-exchange simulated tempering* (REST) [84]. In REST, a short replica-exchange simulation is performed, and the simulated tempering weight factor is determined by the multiple-histogram reweighting techniques [18, 19].

We have introduced two further extensions of REM, which we refer to as *multicanonical replica-exchange method* (MUCAREM) [103, 107, 108] (see also Refs. [131, 132]) and *simulated tempering replica-exchange method* (STREM) [85] (see also Ref. [133] for a similar idea). In MUCAREM, a replica-exchange simulation is performed with a small number of replicas each in multicanonical ensemble of different energy ranges. In STREM, on the other hand, a replica-exchange simulation is performed with a small number of replicas in "simulated tempering" ensemble of different temperature ranges.

Finally, one is naturally led to a multidimensional (or, multivariable) extension of REM, which we refer to as the *multidimensional replica-exhcange method* (MREM) [101]

(see also Refs. [143, 115]). (The method is also referred to as *generalized parallel sampling* [144], *Hamiltonian replica-exchange method* [106], and *Model Hopping*[145].) Some other special cases of MREM can be found in, e.g., Refs. [146, 130, 147, 148, 149, 150, 151]. Another special realization of MREM is *replica-exchange umbrella sampling* (REUS) [101] and it is particularly useful in free energy calculations (see also Ref. [102] for a similar idea). In this article, we just present one of such methods, namely, the replica-exchange method in the isobaric-isothermal ensemble, where not only temperature values but also pressure values are exchanged in the replica-exchange processes [116, 118, 11, 126, 127]. (The results of the first such application of the two-dimensional replica-exchange simulations in the isobaric-isothermal ensemble were presented in Ref. [11].)

In this article, we describe the generalized-ensemble algorithms mentioned above. Namely, we first review the three familiar methods: REM, ST, and MUCA. We then describe various extensions of these methods [101, 152, 153, 154, 155]. Examples of the results by some of these algorithms are then presented.

2 GENERALIZED-ENSEMBLE ALGORITHMS

2.1 Replica-Exchange Method

Let us consider a system of N atoms of mass m_k ($k = 1, \cdots, N$) with their coordinate vectors and momentum vectors denoted by $q \equiv \{\boldsymbol{q}_1, \cdots, \boldsymbol{q}_N\}$ and $p \equiv \{\boldsymbol{p}_1, \cdots, \boldsymbol{p}_N\}$, respectively. The Hamiltonian $H(q, p)$ of the system is the sum of the kinetic energy $K(p)$ and the potential energy $E(q)$:

$$H(q, p) = K(p) + E(q) , \tag{1}$$

where

$$K(p) = \sum_{k=1}^{N} \frac{\boldsymbol{p}_k{}^2}{2m_k} . \tag{2}$$

In the canonical ensemble at temperature T each state $x \equiv (q, p)$ with the Hamiltonian $H(q, p)$ is weighted by the Boltzmann factor:

$$W_{\mathrm{B}}(x; T) = \exp\left(-\beta H(q, p)\right) , \tag{3}$$

where the inverse temperature β is defined by $\beta = 1/k_{\mathrm{B}}T$ (k_{B} is the Boltzmann constant). The average kinetic energy at temperature T is then given by

$$\langle\, K(p)\,\rangle_T = \left\langle \sum_{k=1}^{N} \frac{\boldsymbol{p}_k{}^2}{2m_k} \right\rangle_T = \frac{3}{2} N k_{\mathrm{B}} T . \tag{4}$$

Because the coordinates q and momenta p are decoupled in Eq. (1), we can suppress the kinetic energy part and can write the Boltzmann factor as

$$W_{\mathrm{B}}(x; T) = W_{\mathrm{B}}(E; T) = \exp(-\beta E) . \tag{5}$$

The canonical probability distribution of potential energy $P_{\mathrm{NVT}}(E; T)$ is then given by the product of the density of states $n(E)$ and the Boltzmann weight factor $W_{\mathrm{B}}(E; T)$:

$$P_{\mathrm{NVT}}(E; T) \propto n(E) W_{\mathrm{B}}(E; T) . \tag{6}$$

Because $n(E)$ is a rapidly increasing function and the Boltzmann factor decreases exponentially, the canonical ensemble yields a bell-shaped distribution of potential energy which has a maximum around the average energy at temperature T. The conventional MC or MD simulations at constant temperature are expected to yield $P_{\mathrm{NVT}}(E;T)$. A MC simulation based on the Metropolis algorithm [156] is performed with the following transition probability from a state x of potential energy E to a state x' of potential energy E':

$$w(x \to x') = \min\left(1, \frac{W_{\mathrm{B}}(E';T)}{W_{\mathrm{B}}(E;T)}\right) = \min\left(1, \exp\left(-\beta \Delta E\right)\right) . \tag{7}$$

where

$$\Delta E = E' - E . \tag{8}$$

A MD simulation, on the other hand, is based on the following Newton equations of motion:

$$\dot{\boldsymbol{q}}_k = \frac{\boldsymbol{p}_k}{m_k} , \tag{9}$$

$$\dot{\boldsymbol{p}}_k = -\frac{\partial E}{\partial \boldsymbol{q}_k} = \boldsymbol{f}_k , \tag{10}$$

where $\boldsymbol{f}_k$ is the force acting on the k-th atom $(k = 1, \cdots, N)$. This set of equations actually yield the microcanonical ensemble, however, and we have to add a thermostat in order to obtain the canonical ensemble at temperature T. Here, we just follow Nosé's prescription [157, 158], and we have

$$\dot{\boldsymbol{q}}_k = \frac{\boldsymbol{p}_k}{m_k} , \tag{11}$$

$$\dot{\boldsymbol{p}}_k = -\frac{\partial E}{\partial \boldsymbol{q}_k} - \frac{\dot{s}}{s}\,\boldsymbol{p}_k = \boldsymbol{f}_k - \frac{\dot{s}}{s}\,\boldsymbol{p}_k , \tag{12}$$

$$\dot{s} = s\,\frac{P_s}{Q} , \tag{13}$$

$$\dot{P}_s = \sum_{k=1}^{N} \frac{\boldsymbol{p}_k^{\ 2}}{m_k} - 3Nk_{\mathrm{B}}T = 3Nk_{\mathrm{B}}\left(T(t) - T\right) , \tag{14}$$

where s is Nosé's scaling parameter, P_s is its conjugate momentum, Q is its mass, and the "instantaneous temperature" $T(t)$ is defined by

$$T(t) = \frac{1}{3Nk_{\mathrm{B}}} \sum_{k=1}^{N} \frac{\boldsymbol{p}_k(t)^2}{m_k} . \tag{15}$$

However, in practice, it is very difficult to obtain accurate canonical distributions of complex systems at low temperatures by conventional MC or MD simulation methods. This is because simulations at low temperatures tend to get trapped in one or a few of local-minimum-energy states. This difficulty is overcome by, for instance, the generalized-ensemble algorithms, which greatly enhance conformational sampling.

The *replica-exchange method* (REM) is one of effective generalized-ensemble algorithms. The system for REM consists of M *non-interacting* copies (or, replicas) of the original system in the canonical ensemble at M different temperatures T_m $(m = 1, \cdots, M)$. We arrange the replicas so that there is always exactly one replica at each temperature.

Then there exists a one-to-one correspondence between replicas and temperatures; the label i $(i = 1, \cdots, M)$ for replicas is a permutation of the label m $(m = 1, \cdots, M)$ for temperatures, and vice versa:

$$\begin{cases} i &= i(m) \equiv f(m) , \\ m &= m(i) \equiv f^{-1}(i) , \end{cases} \tag{16}$$

where $f(m)$ is a permutation function of m and $f^{-1}(i)$ is its inverse.

Let $X = \left\{ x_1^{[i(1)]}, \cdots, x_M^{[i(M)]} \right\} = \left\{ x_{m(1)}^{[1]}, \cdots, x_{m(M)}^{[M]} \right\}$ stand for a "state" in this generalized ensemble. Each "substate" $x_m^{[i]}$ is specified by the coordinates $q^{[i]}$ and momenta $p^{[i]}$ of N atoms in replica i at temperature T_m:

$$x_m^{[i]} \equiv \left(q^{[i]}, p^{[i]} \right)_m . \tag{17}$$

Because the replicas are non-interacting, the weight factor for the state X in this generalized ensemble is given by the product of Boltzmann factors for each replica (or at each temperature):

$$\begin{aligned} W_{\mathrm{REM}}(X) &= \prod_{i=1}^{M} \exp \left\{ -\beta_{m(i)} H \left(q^{[i]}, p^{[i]} \right) \right\} = \prod_{m=1}^{M} \exp \left\{ -\beta_m H \left(q^{[i(m)]}, p^{[i(m)]} \right) \right\} , \\ &= \exp \left\{ -\sum_{i=1}^{M} \beta_{m(i)} H \left(q^{[i]}, p^{[i]} \right) \right\} = \exp \left\{ -\sum_{m=1}^{M} \beta_m H \left(q^{[i(m)]}, p^{[i(m)]} \right) \right\} , \end{aligned} \tag{18}$$

where $i(m)$ and $m(i)$ are the permutation functions in Eq. (16).

We now consider exchanging a pair of replicas in this ensemble. Suppose we exchange replicas i and j which are at temperatures T_m and T_n, respectively:

$$X = \left\{ \cdots, x_m^{[i]}, \cdots, x_n^{[j]}, \cdots \right\} \longrightarrow X' = \left\{ \cdots, x_m^{[j]\prime}, \cdots, x_n^{[i]\prime}, \cdots \right\} . \tag{19}$$

Here, i, j, m, and n are related by the permutation functions in Eq. (16), and the exchange of replicas introduces a new permutation function f':

$$\begin{cases} i &= f(m) \longrightarrow j = f'(m) , \\ j &= f(n) \longrightarrow i = f'(n) . \end{cases} \tag{20}$$

The exchange of replicas can be written in more detail as

$$\begin{cases} x_m^{[i]} \equiv \left(q^{[i]}, p^{[i]} \right)_m &\longrightarrow x_m^{[j]\prime} \equiv \left(q^{[j]}, p^{[j]\prime} \right)_m , \\ x_n^{[j]} \equiv \left(q^{[j]}, p^{[j]} \right)_n &\longrightarrow x_n^{[i]\prime} \equiv \left(q^{[i]}, p^{[i]\prime} \right)_n , \end{cases} \tag{21}$$

where the definitions for $p^{[i]\prime}$ and $p^{[j]\prime}$ will be given below. We remark that this process is equivalent to exchanging a pair of temperatures T_m and T_n for the corresponding replicas i and j as follows:

$$\begin{cases} x_m^{[i]} \equiv \left(q^{[i]}, p^{[i]} \right)_m &\longrightarrow x_n^{[i]\prime} \equiv \left(q^{[i]}, p^{[i]\prime} \right)_n , \\ x_n^{[j]} \equiv \left(q^{[j]}, p^{[j]} \right)_n &\longrightarrow x_m^{[j]\prime} \equiv \left(q^{[j]}, p^{[j]\prime} \right)_m . \end{cases} \tag{22}$$

In the original implementation of the *replica-exchange method* (REM) [90]–[92], Monte Carlo algorithm was used, and only the coordinates q (and the potential energy function

$E(q)$) had to be taken into account. In molecular dynamics algorithm, on the other hand, we also have to deal with the momenta p. We proposed the following momentum assignment in Eq. (21) (and in Eq. (22)) [99]:

$$
\begin{cases}
p^{[i]\prime} & \equiv \sqrt{\dfrac{T_n}{T_m}}\, p^{[i]} \,, \\
p^{[j]\prime} & \equiv \sqrt{\dfrac{T_m}{T_n}}\, p^{[j]} \,,
\end{cases}
\tag{23}
$$

which we believe is the simplest and the most natural. This assignment means that we just rescale uniformly the velocities of all the atoms in the replicas by the square root of the ratio of the two temperatures so that the temperature condition in Eq. (4) may be satisfied immediately after replica exchange is accepted.

The transition probability of this replica-exchange process is given by the usual Metropolis criterion:

$$
w(X \to X') \equiv w\left(x_m^{[i]} \mid x_n^{[j]}\right) = \min\left(1, \frac{W_{\mathrm{REM}}(X')}{W_{\mathrm{REM}}(X)}\right) = \min\left(1, \exp\left(-\Delta\right)\right) \,, \tag{24}
$$

where in the second expression (i.e., $w(x_m^{[i]}|x_n^{[j]})$) we explicitly wrote the pair of replicas (and temperatures) to be exchanged. From Eqs. (1), (2), (18), and (23), we have

$$
\begin{aligned}
\frac{W_{\mathrm{REM}}(X')}{W_{\mathrm{REM}}(X)} &= \exp\left\{-\beta_m\left[K\left(p^{[j]\prime}\right) + E\left(q^{[j]}\right)\right] - \beta_n\left[K\left(p^{[i]\prime}\right) + E\left(q^{[i]}\right)\right]\right. \\
&\quad \left. + \beta_m\left[K\left(p^{[i]}\right) + E\left(q^{[i]}\right)\right] + \beta_n\left[K\left(p^{[j]}\right) + E\left(q^{[j]}\right)\right]\right\} \,, \\
&= \exp\left\{-\beta_m\frac{T_m}{T_n}K\left(p^{[j]}\right) - \beta_n\frac{T_n}{T_m}K\left(p^{[i]}\right) + \beta_m K\left(p^{[i]}\right) + \beta_n K\left(p^{[j]}\right)\right. \\
&\quad \left. - \beta_m\left[E\left(q^{[j]}\right) - E\left(q^{[i]}\right)\right] - \beta_n\left[E\left(q^{[i]}\right) - E\left(q^{[j]}\right)\right]\right\} \,.
\end{aligned}
\tag{25}
$$

Because the kinetic energy terms in this equation all cancel out, Δ in Eq. (24) becomes

$$
\begin{aligned}
\Delta &= \beta_m\left(E\left(q^{[j]}\right) - E\left(q^{[i]}\right)\right) - \beta_n\left(E\left(q^{[j]}\right) - E\left(q^{[i]}\right)\right) \,, \tag{26} \\
&= (\beta_m - \beta_n)\left(E\left(q^{[j]}\right) - E\left(q^{[i]}\right)\right) \,. \tag{27}
\end{aligned}
$$

Here, i, j, m, and n are related by the permutation functions in Eq. (16) before the replica exchange:

$$
\begin{cases}
i & = f(m) \,, \\
j & = f(n) \,.
\end{cases}
\tag{28}
$$

Note that after introducing the momentum rescaling in Eq. (23), we have the same Metropolis criterion for replica exchanges, i.e., Eqs. (24) and (27), for both MC and MD versions.

Without loss of generality we can assume $T_1 < T_2 < \cdots < T_M$. The lowest temperature T_1 should be sufficiently low so that the simulation can explore the global-minimum-energy region, and the highest temperature T_M should be sufficiently high so that no trapping in an energy-local-minimum state occurs. A simulation of the *replica-exchange method* (REM) is then realized by alternately performing the following two steps:

1. Each replica in canonical ensemble of the fixed temperature is simulated *simultaneously* and *independently* for a certain MC or MD steps.

2. A pair of replicas at neighboring temperatures, say $x_m^{[i]}$ and $x_{m+1}^{[j]}$, are exchanged with the probability $w\left(x_m^{[i]} \mid x_{m+1}^{[j]}\right)$ in Eq. (24).

Note that in Step 2 we exchange only pairs of replicas corresponding to neighboring temperatures, because the acceptance ratio of the exchange process decreases exponentially with the difference of the two β's (see Eqs. (27) and (24)). Note also that whenever a replica exchange is accepted in Step 2, the permutation functions in Eq. (16) are updated. A random walk in "temperature space" is realized for each replica, which in turn induces a random walk in potential energy space. This alleviates the problem of getting trapped in states of energy local minima.

The REM simulation is particularly suitable for parallel computers. Because one can minimize the amount of information exchanged among nodes, it is best to assign each replica to each node (exchanging pairs of temperature values among nodes is much faster than exchanging coordinates and momenta). This means that we keep track of the permutation function $m(i;t) = f^{-1}(i;t)$ in Eq. (16) as a function of MC or MD step t during the simulation. After parallel canonical MC or MD simulations for a certain steps (Step 1), $M/2$ pairs of replicas corresponding to neighboring temperatures are simulateneously exchanged (Step 2), and the pairing is alternated between the two possible choices, i.e., $(T_1, T_2), (T_3, T_4), \cdots$ and $(T_2, T_3), (T_4, T_5), \cdots$.

After a long production run of a replica-exchange simulation, the canonical expectation value of a physical quantity A at temperature T_m $(m = 1, \cdots, M)$ can be calculated by the usual arithmetic mean:

$$< A >_{T_m} = \frac{1}{n_m} \sum_{k=1}^{n_m} A\left(x_m(k)\right) , \tag{29}$$

where $x_m(k)$ $(k = 1, \cdots, n_m)$ are the configurations obtained at temperature T_m and n_m is the total number of measurements made at $T = T_m$. The expectation value at any intermediate temperature T $(= 1/k_B\beta)$ can also be obtained as follows:

$$< A >_T = \frac{\sum_E A(E) P_{\mathrm{NVT}}(E;T)}{\sum_E P_{\mathrm{NVT}}(E;T)} = \frac{\sum_E A(E) n(E) \exp(-\beta E)}{\sum_E n(E) \exp(-\beta E)} . \tag{30}$$

The summation instead of integration is used in Eq. (30), because we often discretize the potential energy E with step size ϵ $(E = E_i; i = 1, 2, \cdots)$. Here, the explicit form of the physical quantity A should be known as a function of potential energy E. For instance, $A(E) = E$ gives the average potential energy $< E >_T$ as a function of temperature, and $A(E) = \beta^2(E - < E >_T)^2$ gives specific heat.

The density of states $n(E)$ in Eq. (30) is given by the multiple-histogram reweighting techniques [18, 19] as follows. Let $N_m(E)$ and n_m be respectively the potential-energy histogram and the total number of samples obtained at temperature $T_m = 1/k_B\beta_m$ $(m = 1, \cdots, M)$. The best estimate of the density of states is then given by [18, 19]

$$n(E) = \frac{\sum_{m=1}^{M} g_m^{-1} N_m(E)}{\sum_{m=1}^{M} g_m^{-1} n_m \exp(f_m - \beta_m E)} , \tag{31}$$

where we have for each $m \ (= 1, \cdots, M)$

$$\exp(-f_m) = \sum_E \ n(E) \ \exp(-\beta_m E) \ . \tag{32}$$

Here, $g_m = 1 + 2\tau_m$, and τ_m is the integrated autocorrelation time at temperature T_m. For many systems the quantity g_m can safely be set to be a constant in the reweighting formulae [19], and hereafter we set $g_m = 1$.

Note that Eqs. (31) and (32) are solved self-consistently by iteration [18, 19] to obtain the density of states $n(E)$ and the dimensionless Helmholtz free energy f_m. Namely, we can set all the $f_m \ (m = 1, \cdots, M)$ to, e.g., zero initially. We then use Eq. (31) to obtain $n(E)$, which is substituted into Eq. (32) to obtain next values of f_m, and so on.

Moreover, the ensemble averages of any physical quantity A (including those that cannot be expressed as functions of potential energy) at any temperature $T \ (= 1/k_{\rm B}\beta)$ can now be obtained from the "trajectory" of configurations of the production run. Namely, we first obtain $f_m \ (m = 1, \cdots, M)$ by solving Eqs. (31) and (32) self-consistently, and then we have [107] (see also [159])

$$< A >_T = \frac{\displaystyle\sum_{m=1}^{M} \sum_{k=1}^{n_m} A(x_m(k)) \frac{1}{\displaystyle\sum_{\ell=1}^{M} n_\ell \exp\left[f_\ell - \beta_\ell E(x_m(k))\right]} \exp\left[-\beta E(x_m(k))\right]}{\displaystyle\sum_{m=1}^{M} \sum_{k=1}^{n_m} \frac{1}{\displaystyle\sum_{\ell=1}^{M} n_\ell \exp\left[f_\ell - \beta_\ell E(x_m(k))\right]} \exp\left[-\beta E(x_m(k))\right]} \ , \tag{33}$$

where $x_m(k) \ (k = 1, \cdots, n_m)$ are the configurations obtained at temperature T_m.

Eqs. (30) and (31) or any other equations which involve summations of exponential functions often encounter with numerical difficulties such as overflows. These can be overcome by using, for instance, the following equation [22, 160]: For $C = A + B$ (with $A > 0$ and $B > 0$) we have

$$\begin{aligned}
\ln C \ &= \ln\left[\max(A, B)\left(1 + \frac{\min(A, B)}{\max(A, B)}\right)\right] \ , \\
&= \max(\ln A, \ln B) + \ln\left\{1 + \exp\left[\min(\ln A, \ln B) - \max(\ln A, \ln B)\right]\right\} \ .
\end{aligned} \tag{34}$$

We now give more details about the momentum rescaling in Eq. (23) [161]. Actually, Eq. (23) is only valid for the Langevin dynamics [162], Andersen thermostat [163], and Gaussian constraint method [164, 165, 166]. The former two thermostats are based on the weight factor of Eq. (3) with Eqs. (1) and (2), and the Gaussian contraint method is based on the following weight factor:

$$W(q, p) = \delta\left(\sum_{k=1}^{N} \frac{\boldsymbol{p}_k^2}{2m_k} - \frac{g k_{\rm B} T}{2}\right) \exp\left[-\beta E(q)\right] \ . \tag{35}$$

For Nosé's method [157, 158], which gives the equations of motion in Eqs. (11)–(14), the Nosé Hamiltonian is given by

$$H_{\rm Nose} = \sum_{k=1}^{N} \frac{\tilde{\boldsymbol{p}}_k^2}{2m_k s^2} + E(q) + \frac{P_s^2}{2Q} + g k_{\rm B} T \log s. \tag{36}$$

Here, $g \ (= 3N)$ is the number of degrees of freedom, s is a position variable of the thermostat, P_s is a momentum conjugate to s, and $\tilde{\boldsymbol{p}}_k$ is a virtual momentum, which is related to the real momenta $\boldsymbol{p}_k$ as $\boldsymbol{p}_k = \tilde{\boldsymbol{p}}_k/s$. The weight factor for the Nosé's method is then given by

$$W(q, \tilde{p}, s, P_s) = \delta \left(H_{\mathrm{Nose}} - \mathcal{E} \right) , \tag{37}$$

where $\mathcal{E}$ is the initial value of H_{Nose}. Namely, in the Nosé's method, the entire system including the thermostat is in the microcanonical ensemble. Note that the mass Q of the thermostat can have different values in each replica in REMD simulations. The rescaling method for the Nosé thermostat is given by Eq. (23) and

$$P_s^{[i]\prime} = \sqrt{\frac{T_n Q_n}{T_m Q_m}} P_s^{[i]}, \quad P_s^{[j]\prime} = \sqrt{\frac{T_m Q_m}{T_n Q_n}} P_s^{[j]}, \tag{38}$$

$$
\begin{aligned}
s^{[i]\prime} &= s^{[i]} \exp \left[\frac{1}{g k_{\mathrm{B}}} \left(\frac{E(q^{[i]}) - \mathcal{E}_m}{T_m} - \frac{E(q^{[i]}) - \mathcal{E}_n}{T_n} \right) \right], \\
s^{[j]\prime} &= s^{[j]} \exp \left[\frac{1}{g k_{\mathrm{B}}} \left(\frac{E(q^{[j]}) - \mathcal{E}_n}{T_n} - \frac{E(q^{[j]}) - \mathcal{E}_m}{T_m} \right) \right],
\end{aligned}
\tag{39}
$$

where $\mathcal{E}_m$ and $\mathcal{E}_n$ are the initial values of H_{Nose} in the simulations with T_m and T_n, respectively, before the replica exchange. Note that the real momenta have to be used in the rescaling method in Eq. (23), not the virtual momenta.

For the Nosé-Hoover thermostat [167], the states are specified by the following weight factor:

$$W(q, p, \zeta) = \exp \left[-\beta \left(\sum_{k=1}^{N} \frac{\boldsymbol{p}_k^2}{2m_k} + E(q) + \frac{Q}{2} \zeta^2 \right) \right], \tag{40}$$

where ζ is a velocity of the thermostat and Q is its mass parameter. The rescaling method for the Nosé-Hoover thermostat is given by Eq. (23) and

$$\zeta^{[i]\prime} = \sqrt{\frac{T_n Q_m}{T_m Q_n}} \zeta^{[i]}, \quad \zeta^{[j]\prime} = \sqrt{\frac{T_m Q_n}{T_n Q_m}} \zeta^{[j]}, \tag{41}$$

where Q_m and Q_n are the mass parameters in the replicas at temperature values T_m and T_n, respectively, before the replica exchange.

The rescaling method for the Nosé-Hoover thermostat can be generalized to the Nosé-Hoover chains [168] in a similar way. The weight factor for the Nosé-Hoover chains is given by

$$W(q, p, \zeta_1, \cdots, \zeta_{\mathcal{L}}) = \exp \left[-\beta \left(\sum_{k=1}^{N} \frac{\boldsymbol{p}_k^2}{2m_k} + E(q) + \sum_{\ell=1}^{\mathcal{L}} \frac{Q_\ell}{2} \zeta_\ell^2 \right) \right], \tag{42}$$

where $\mathcal{L}$ is the number of thermostats, $\zeta_\ell \ (\ell = 1, \cdots, \mathcal{L})$ is the velocity of the ℓ-th thermostat, and $Q_\ell \ (\ell = 1, \cdots, \mathcal{L})$ is a mass parameter corresponding to the ℓ-th thermostat. A rescaling method for REMD with the Nosé-Hoover chains is given by Eq. (23) and the following:

$$\zeta_\ell^{[i]\prime} = \sqrt{\frac{T_n Q_{m,\ell}}{T_m Q_{n,\ell}}} \zeta_\ell^{[i]}, \quad \zeta_\ell^{[j]\prime} = \sqrt{\frac{T_m Q_{n,\ell}}{T_n Q_{m,\ell}}} \zeta_\ell^{[j]}, \ (\ell = 1, \cdots, \mathcal{L}), \tag{43}$$

where $Q_{m,\ell}$ and $Q_{n,\ell}$ are the mass parameters in the replicas at temperature values T_m and T_n, respectively, which correspond to the ℓ-th thermostat.

In the Nosé-Poincaré thermostat [169], the states are specified by $x \equiv (q, \tilde{p}, s, P_s)$ and the weight factor is given by

$$W(q, \tilde{p}, s, P_s) \propto \delta \left[s \left(H_{\text{Nose}} - \mathcal{E} \right) \right] , \tag{44}$$

where H_{Nose} is the Nosé Hamiltonian in Eq. (36) and $\mathcal{E}$ is its initial value. A rescaling method of the Nosé-Poincaré thermostat is the same as in the Nosé's thermostat and given by Eqs. (23), (38), and (39) above.

2.2 Simulated Tempering

We now introduce another generalized-ensemble algorithm, the *simulated tempering* (ST) method [78, 79]. In this method temperature itself becomes a dynamical variable, and both the configuration and the temperature are updated during the simulation with a weight:

$$W_{\text{ST}}(E; T) = \exp \left(-\beta E + a(T) \right) , \tag{45}$$

where the function $a(T)$ is chosen so that the probability distribution of temperature is flat:

$$P_{\text{ST}}(T) = \int dE \, n(E) \, W_{\text{ST}}(E; T) = \int dE \, n(E) \, \exp \left(-\beta E + a(T) \right) = \text{constant} . \tag{46}$$

Hence, in simulated tempering, *temperature* is sampled uniformly. A free random walk in temperature space is realized, which in turn induces a random walk in potential energy space and allows the simulation to escape from states of energy local minima.

In the numerical work we discretize the temperature in M different values, T_m ($m = 1, \cdots, M$). Without loss of generality we can order the temperature so that $T_1 < T_2 < \cdots < T_M$. The probability weight factor in Eq. (45) is now written as

$$W_{\text{ST}}(E; T_m) = \exp(-\beta_m E + a_m) , \tag{47}$$

where $a_m = a(T_m)$ ($m = 1, \cdots, M$). Note that from Eqs. (46) and (47) we have

$$\exp(-a_m) \propto \int dE \, n(E) \, \exp(-\beta_m E) . \tag{48}$$

The parameters a_m are therefore "dimensionless" Helmholtz free energy at temperature T_m (i.e., the inverse temperature β_m multiplied by the Helmholtz free energy).

Once the parameters a_m are determined and the initial configuration and the initial temperature T_m are chosen, a simulated tempering simulation is realized by alternately performing the following two steps [78, 79]:

1. A canonical MC or MD simulation at the fixed temperature T_m is carried out for a certain steps.

2. The temperature T_m is updated to the neighboring values $T_{m\pm1}$ with the configuration fixed. The transition probability of this temperature-updating process is given by the following Metropolis criterion (see Eq. (47)):

$$w(T_m \to T_{m\pm1}) = \min \left(1, \frac{W_{\text{ST}}(E; T_{m\pm1})}{W_{\text{ST}}(E; T_m)} \right) = \min \left(1, \exp \left(-\Delta \right) \right) , \tag{49}$$

where

$$\Delta = (\beta_{m\pm1} - \beta_m) E - (a_{m\pm1} - a_m) . \tag{50}$$

Note that in Step 2 we update the temperature only to the neighboring temperatures in order to secure sufficiently large acceptance ratio of temperature updates.

We remark that when MD simulations are performed in Step 1 above, we also have to deal with the momenta p, and the kinetic energy term should be included in the weight factor. When temperature $T_{m_0 \pm 1}$ is accepted for T-update in Step 2, we rescale the momenta in the same way as in REMD [99, 153, 155]:

$$\boldsymbol{p}_k{}' = \sqrt{\frac{T_{m_0 \pm 1}}{T_{m_0}}} \; \boldsymbol{p}_k \; . \tag{51}$$

The kinetic energy terms then cancel out in Eq. (50) and we can use the same Δ in the Metropolis criterion in Step 2 for both MC and MD simulations. Similar momentum scaling formulae given above should also be introduced for various other thermostats [161].

The simulated tempering parameters $a_m = a(T_m)$ $(m = 1, \cdots, M)$ can be determined by iterations of short trial simulations (see, e.g., Refs. [80, 82, 50] for details). This process can be non-trivial and very tedius for complex systems.

After the optimal simulated tempering weight factor is determined, one performs a long simulated tempering run once. The canonical expectation value of a physical quantity A at temperature T_m $(m = 1, \cdots, M)$ can be calculated by the usual arithmetic mean from Eq. (29). The expectation value at any intermediate temperature can also be obtained from Eq. (30), where the density of states is given by the multiple-histogram reweighting techniques [18, 19]. Namely, let $N_m(E)$ and n_m be respectively the potential-energy histogram and the total number of samples obtained at temperature $T_m = 1/k_{\mathrm{B}}\beta_m$ $(m = 1, \cdots, M)$. The best estimate of the density of states is then given by solving Eqs. (31) and (32) self-consistently.

Moreover, the ensemble averages of any physical quantity A (including those that cannot be expressed as functions of potential energy) at any temperature T $(= 1/k_{\mathrm{B}}\beta)$ can now be obtained from Eq. (33).

2.3 Multicanonical Algorithm

The third generalized-ensemble algorithm that we present is the *multicanonical algorithm* (MUCA) [20, 21]. In the multicanonical ensemble, each state is weighted by a non-Boltzmann weight factor $W_{\mathrm{MUCA}}(E)$ (which we refer to as the *multicanonical weight factor*) so that a uniform potential energy distribution $P_{\mathrm{MUCA}}(E)$ is obtained:

$$P_{\mathrm{MUCA}}(E) \propto n(E) W_{\mathrm{MUCA}}(E) \equiv \text{constant} \; . \tag{52}$$

The flat distribution implies that a free one-dimensional random walk in the potential energy space is realized in this ensemble. This allows the simulation to escape from any local minimum-energy states and to sample the configurational space much more widely than the conventional canonical MC or MD methods.

The definition in Eq. (52) implies that the multicanonical weight factor is inversely proportional to the density of states, and we can write it as follows:

$$W_{\mathrm{MUCA}}(E) \equiv \exp\left[-\beta_a E_{\mathrm{MUCA}}(E; T_a)\right] = \frac{1}{n(E)} \; , \tag{53}$$

where we have chosen an arbitrary reference temperature, $T_a = 1/k_B \beta_a$, and the "*multicanonical potential energy*" is defined by

$$E_{\text{MUCA}}(E; T_a) \equiv k_B T_a \ln n(E) = T_a S(E) . \tag{54}$$

Here, $S(E)$ is the entropy in the microcanonical ensemble. Because the density of states of the system is usually unknown, the multicanonical weight factor has to be determined numerically by iterations of short preliminary runs [20, 21].

A multicanonical MC simulation is performed, for instance, with the usual Metropolis criterion [156]: The transition probability of state x with potential energy E to state x' with potential energy E' is given by

$$w(x \to x') = \min \left(1, \frac{W_{\text{MUCA}}(E')}{W_{\text{MUCA}}(E)} \right) = \min \left(1, \frac{n(E)}{n(E')} \right) = \min \left(1, \exp \left(-\beta_a \Delta E_{\text{MUCA}} \right) \right) , \tag{55}$$

where

$$\Delta E_{\text{MUCA}} = E_{\text{MUCA}}(E'; T_a) - E_{\text{MUCA}}(E; T_a) . \tag{56}$$

The MD algorithm in the multicanonical ensemble also naturally follows from Eq. (53), in which the regular constant temperature MD simulation (with $T = T_a$) is performed by replacing E by E_{MUCA} in Eq. (12) [48, 52]:

$$\dot{\boldsymbol{p}}_k = -\frac{\partial E_{\text{MUCA}}(E; T_a)}{\partial \boldsymbol{q}_k} - \frac{\dot{s}}{s} \, \boldsymbol{p}_k = \frac{\partial E_{\text{MUCA}}(E; T_a)}{\partial E} \, \boldsymbol{f}_k - \frac{\dot{s}}{s} \, \boldsymbol{p}_k . \tag{57}$$

If the exact multicanonical weight factor $W_{\text{MUCA}}(E)$ is known, one can calculate the ensemble averages of any physical quantity A at any temperature $T \, (= 1/k_B \beta)$ from Eq. (30), where the density of states is given by (see Eq. (53))

$$n(E) = \frac{1}{W_{\text{MUCA}}(E)} . \tag{58}$$

In general, the multicanonical weight factor $W_{\text{MUCA}}(E)$, or the density of states $n(E)$, is not *a priori* known, and one needs its estimator for a numerical simulation. This estimator is usually obtained from iterations of short trial multicanonical simulations. The details of this process are described, for instance, in Refs. [34, 43]. However, the iterative process can be non-trivial and very tedius for complex systems.

In practice, it is impossible to obtain the ideal multicanonical weight factor with completely uniform potential energy distribution. The question is when to stop the iteration for the weight factor determination. Our criterion for a satisfactory weight factor is that as long as we do get a random walk in potential energy space, the probability distribution $P_{\text{MUCA}}(E)$ does not have to be completely flat with a tolerance of, say, an order of magnitude deviation. In such a case, we usually perform with this weight factor a multicanonical simulation with high statistics (production run) in order to get even better estimate of the density of states. Let $N_{\text{MUCA}}(E)$ be the histogram of potential energy distribution $P_{\text{MUCA}}(E)$ obtained by this production run. The best estimate of the density of states can then be given by the single-histogram reweighting techniques [17] as follows (see the proportionality relation in Eq. (52)):

$$n(E) = \frac{N_{\text{MUCA}}(E)}{W_{\text{MUCA}}(E)} . \tag{59}$$

By substituting this quantity into Eq. (30), one can calculate ensemble averages of physical quantity $A(E)$ as a function of temperature. Moreover, the ensemble averages of any physical quantity A (including those that cannot be expressed as functions of potential energy) at any temperature T $(= 1/k_{\mathrm{B}}\beta)$ can also be obtained as long as one stores the "trajectory" of configurations from the production run. Namely, we have

$$
< A >_T = \frac{\displaystyle\sum_{k=1}^{n_s} A(x_k) W_{\mathrm{MUCA}}^{-1}(E(x_k)) \exp\left[-\beta E(x_k)\right]}{\displaystyle\sum_{k=1}^{n_s} W_{\mathrm{MUCA}}^{-1}(E(x_k)) \exp\left[-\beta E(x_k)\right]} \ , \tag{60}
$$

where x_k is the configuration at the k-th MC (or MD) step and n_s is the total number of configurations stored. Note that when A is a function of E, Eq. (60) reduces to Eq. (30) where the density of states is given by Eq. (59).

Some remarks are in order. The major advantage of REM over other generalized-ensemble methods such as simulated tempering [78, 79] and multicanonical algorithm [20, 21] lies in the fact that the weight factor is *a priori* known (see Eq. (18)), while in simulated tempering and multicanonical algorithm the determination of the weight factors can be very tedius and time-consuming. In REM, however, the number of required replicas increases greatly ($\propto \sqrt{N}$) as the system size N increases [90], while only one replica is used in simulated tempering and multicanonical algorithm. This demands a lot of computer power for complex systems. Moreover, so long as optimal weight factors can be obtained, simulated tempering and multicanonical algorithm are more efficient in sampling than the replica-exchange method [15, 85, 108, 75].

2.4 Replica-Exchange Simulated Tempering and Replica-Exchange Multicanonical Algorithm

The *replica-exchange simulated tempering* (REST) [84] and the *replica-exchange multi-canonical algorithm* (REMUCA) [103, 107, 108] overcome both the difficulties of ST and MUCA (the weight factor determinations are non-trivial) and REM (many replicas, or a lot of computation time, are required).

In REST [84], we first perform a short REM simulation (with M replicas) to determine the simulated tempering weight factor and then perform with this weight factor a regular ST simulation with high statistics. The first step is accomplished by the multiple-histogram reweighting techniques [18, 19], which give the dimensionless Helmholtz free energy. Let $N_m(E)$ and n_m be respectively the potential-energy histogram and the total number of samples obtained at temperature T_m $(= 1/k_{\mathrm{B}}\beta_m)$ of the REM run. The dimensionless Helmholtz free energy f_m is then given by solving Eqs. (31) and (32) self-consistently by iteration.

Once the estimate of the dimensionless Helmholtz free energy f_m are obtained, the simulated tempering weight factor can be directly determined by using Eq. (47) where we set $a_m = f_m$ (compare Eq. (48) with Eq. (32)). A long simulated tempering run is then performed with this weight factor. Let $N_m(E)$ and n_m be respectively the potential-energy histogram and the total number of samples obtained at temperature T_m $(= 1/k_{\mathrm{B}}\beta_m)$ from this simulated tempering run. The multiple-histogram reweighting techniques of Eqs. (31) and (32) can be used again to obtain the best estimate of the density of states $n(E)$. The

14

expectation value of a physical quantity A at any temperature T $(= 1/k_B\beta)$ is then calculated from Eq. (30).

We now present the *replica-exchange multicanonical algorithm* (REMUCA) [103, 107, 108]. In REMUCA, just as in REST, we first perform a short REM simulation (with M replicas) to determine the multicanonical weight factor and then perform with this weight factor a regular multicanonical simulation with high statistics. The first step is accomplished by the multiple-histogram reweighting techniques [18, 19], which give the density of states. Let $N_m(E)$ and n_m be respectively the potential-energy histogram and the total number of samples obtained at temperature T_m $(= 1/k_B\beta_m)$ of the REM run. The density of states $n(E)$ is then given by solving Eqs. (31) and (32) self-consistently by iteration.

Once the estimate of the density of states is obtained, the multicanonical weight factor can be directly determined from Eq. (53) (see also Eq. (54)). Actually, the density of states $n(E)$ and the multicanonical potential energy, $E_{\mathrm{MUCA}}(E; T_0)$, thus determined are only reliable in the following range:

$$E_1 \leq E \leq E_M , \tag{61}$$

where

$$\begin{cases} E_1 &= <E>_{T_1} , \\ E_M &= <E>_{T_M} , \end{cases} \tag{62}$$

and T_1 and T_M are respectively the lowest and the highest temperatures used in the REM run. Outside this range we extrapolate the multicanonical potential energy linearly [103]:

$$\mathcal{E}_{\mathrm{MUCA}}(E) \equiv \begin{cases} \left.\dfrac{\partial E_{\mathrm{MUCA}}(E; T_0)}{\partial E}\right|_{E=E_1} (E - E_1) + E_{\mathrm{MUCA}}(E_1; T_0) , & \text{for } E < E_1, \\ E_{\mathrm{MUCA}}(E; T_0) , & \text{for } E_1 \leq E \leq E_M, \\ \left.\dfrac{\partial E_{\mathrm{MUCA}}(E; T_0)}{\partial E}\right|_{E=E_M} (E - E_M) + E_{\mathrm{MUCA}}(E_M; T_0) , & \text{for } E > E_M. \end{cases} \tag{63}$$

For Monte Carlo method, the weight factor for REMUCA is given by substituting Eq. (63) into Eq. (53) [103, 107]:

$$W_{\mathrm{MUCA}}(E) = \exp\left[-\beta_0 \mathcal{E}_{\mathrm{MUCA}}(E)\right] = \begin{cases} \exp\left(-\beta_1 E\right) , & \text{for } E < E_1, \\ \dfrac{1}{n(E)} , & \text{for } E_1 \leq E \leq E_M, \\ \exp\left(-\beta_M E\right) , & \text{for } E > E_M. \end{cases} \tag{64}$$

The multicanonical MC and MD runs are then performed respectively with the Metropolis criterion of Eq. (55) and with the modified Newton equation in Eq. (57), in which $\mathcal{E}_{\mathrm{MUCA}}(E)$ in Eq. (63) is substituted into $E_{\mathrm{MUCA}}(E; T_0)$. We expect to obtain a flat potential energy distribution in the range of Eq. (61). Finally, the results are analyzed by the single-histogram reweighting techniques as described in Eq. (59) (and Eq. (30)).

The formulations of REST and REMUCA are simple and straightforward, but the numerical improvement is great, because the weight factor determination for ST and MUCA becomes very difficult by the usual iterative processes for complex systems.

2.5 Simulated Tempering Replica-Exchange Method and Multicanonical Replica-Exchange Method

In the previous subsection we presented REST and REMUCA, which use a short REM run for the determination of the simulated temepering weight factor and the multicanonical weight factor, respectively. Here, we present two modifications of REM and refer to the new methods as the *simulated tempering replica-exchange method* (STREM) [85] and *multicanonical replica-exchange method* (MUCAREM) [103, 107, 108]. In STREM the production run is a REM simulation with a few replicas that perform ST simulations with different temperature ranges. Likewise, in MUCAREM the production run is a REM simulation with a few replicas in multicanonical ensembles, i.e., different replicas perform MUCA simulations with different energy ranges.

While ST and MUCA simulations are usually based on local updates, a replica-exchange process can be considered to be a global update, and global updates enhance the conformational sampling further.

3 MULTIDIMENSIONAL EXTENSIONS OF THE THREE GENERALIZED-ENSEMBLE ALGORITHMS

3.1 General Formulations

We now give the general formulations for the multidimensional generalized-ensemble algorithms [152, 153, 154]. Let us consider a generalized potential energy function $E_{\boldsymbol{\lambda}}(x)$, which depends on L parameters $\boldsymbol{\lambda} = (\lambda^{(1)}, \cdots, \lambda^{(L)})$, of a system in state x. Although $E_{\boldsymbol{\lambda}}(x)$ can be any function of $\boldsymbol{\lambda}$, we consider the following specific generalized potential energy function for simplicity:

$$E_{\boldsymbol{\lambda}}(x) = E_0(x) + \sum_{\ell=1}^{L} \lambda^{(\ell)} V_\ell(x) \ . \tag{65}$$

Here, there are $L + 1$ energy terms, $E_0(x)$ and $V_\ell(x)$ $(\ell = 1, \cdots, L)$, and $\lambda^{(\ell)}$ are the corresponding coupling constants for $V_\ell(x)$.

After integrating out the momentum degrees of freedom, the partition function of the system at fixed temperature T and parameters $\boldsymbol{\lambda}$ is given by

$$Z(T, \boldsymbol{\lambda}) = \int dx \exp(-\beta E_{\boldsymbol{\lambda}}(x)) = \int dE_0 dV_1 \cdots dV_L \ n(E_0, V_1, \cdots, V_L) \exp\left(-\beta E_{\boldsymbol{\lambda}}\right) \ , \tag{66}$$

where $n(E_0, V_1, \cdots, V_L)$ is the multidimensional density of states:

$$n(E_0, V_1, \cdots, V_L) = \int dx \delta(E_0(x) - E_0)\delta(V_1(x) - V_1)\cdots\delta(V_L(x) - V_L) \ . \tag{67}$$

Here, the integration is replaced by a summation when x is discrete.

The expression in Eq. (65) is often used in simulations. For instance, in simulations of spin systems, $E_0(x)$ and $V_1(x)$ (here, $L = 1$ and $x = \{S_1, S_2, \cdots\}$ stand for spins) can be respectively considered as the zero-field term and the magnetization term coupled with the external field $\lambda^{(1)}$. (For Ising model, $E_0 = -J \sum_{<i,j>} S_i S_j$, $V_1 = -\sum_i S_i$, and $\lambda^{(1)} = h$, i.e.,

external magnetic field.) In umbrella sampling [28] in molecular simulations, $E_0(x)$ and $V_\ell(x)$ can be taken as the original potential energy and the (biasing) umbrella potential energy, respectively, with the coupling parameter $\lambda^{(\ell)}$ (here, $x = \{\boldsymbol{q}_1, \cdots, \boldsymbol{q}_N\}$ where $\boldsymbol{q}_k$ is the coordinate vector of the k-th particle and N is the total number of particles). For the molecular simulations in the isobaric-isothermal ensemble, $E_0(x)$ and $V_1(x)$ (here, $L = 1$) correspond respectively to the potential energy U and the volume $\mathcal{V}$ coupled with the pressure $\mathcal{P}$. (Namely, we have $x = \{\boldsymbol{q}_1, \cdots, \boldsymbol{q}_N, \mathcal{V}\}$, $E_0 = U$, $V_1 = \mathcal{V}$, and $\lambda^{(1)} = \mathcal{P}$, i.e., $E_{\boldsymbol{\lambda}}$ is the enthalpy without the kinetic energy contributions.) For simulations in the grand canonical ensemble with N particles, we have $x = \{\boldsymbol{q}_1, \cdots, \boldsymbol{q}_N, N\}$, and $E_0(x)$ and $V_1(x)$ (here, $L = 1$) correspond respectively to the potential energy U and the total number of particles N coupled with the chemical potential μ. (Namely, we have $E_0 = U$, $V_1 = N$, and $\lambda^{(1)} = -\mu$.)

Moreover, going beyond the well-known ensembles discussed above, we can introduce any physical quantity of interest (or its function) as the additional potential energy term V_ℓ. For instance, V_ℓ can be an overlap with a reference configuration in spin glass systems, an end-to-end distance, a radius of gyration in molecular systems, etc. In such a case, we have to carefully choose the range of $\lambda^{(\ell)}$ values so that the new energy term $\lambda^{(\ell)}V_\ell$ will have roughly the same order of magnitude as the original energy term E_0. We want to perform a simulation where a random walk not only in the E_0 space but also in the V_ℓ space is realized. As shown below, this can be done by performing a multidimensional REM, ST, or MUCA simulation.

We first describe the *multidimensional replica-exchange method* (MREM) [101]. The crucial observation that led to this algorithm is: As long as we have M *non-interacting* replicas of the original system, the Hamiltonian $H(q, p)$ of the system does not have to be identical among the replicas and it can depend on a parameter with different parameter values for different replicas. The system for the multidimensional REM consists of M non-interacting replicas of the original system in the "canonical ensemble" with $M(= M_0 \times M_1 \times \cdots \times M_L)$ different parameter sets $\boldsymbol{\Lambda}_m$ $(m = 1, \cdots, M)$, where $\boldsymbol{\Lambda}_m \equiv (T_{m_0}, \boldsymbol{\lambda}_m) \equiv (T_{m_0}, \lambda_{m_1}^{(1)}, \cdots, \lambda_{m_L}^{(L)})$ with $m_0 = 1, \cdots, M_0, m_\ell = 1, \cdots, M_\ell$ $(\ell = 1, \cdots, L)$. Because the replicas are non-interacting, the weight factor is given by the product of Boltzmann-like factors for each replica:

$$W_{\mathrm{MREM}} \equiv \prod_{m_0=1}^{M_0} \prod_{m_1=1}^{M_1} \cdots \prod_{m_L=1}^{M_L} \exp\left(-\beta_{m_0} E_{\boldsymbol{\lambda}_m}\right). \tag{68}$$

Without loss of generality we can order the parameters so that $T_1 < T_2 < \cdots < T_{M_0}$ and $\lambda_1^{(\ell)} < \lambda_2^{(\ell)} < \cdots < \lambda_{M_\ell}^{(\ell)}$ (for each $\ell = 1, \cdots, L$). The multidimensional REM is realized by alternately performing the following two steps:

1. For each replica, a "canonical" MC or MD simulation at the fixed parameter set is carried out simultaneously and independently for a certain steps.

2. We exchange a pair of replicas i and j which are at the parameter sets $\boldsymbol{\Lambda}_m$ and $\boldsymbol{\Lambda}_{m+1}$, respectively. The transition probability for this replica exchange process is given by

$$w(\boldsymbol{\Lambda}_m \leftrightarrow \boldsymbol{\Lambda}_{m+1}) = \min\left(1, \exp(-\Delta)\right), \tag{69}$$

where we have

$$\Delta = (\beta_{m_0} - \beta_{m_0+1})\left(E_{\boldsymbol{\lambda}_m}\left(q^{[j]}\right) - E_{\boldsymbol{\lambda}_m}\left(q^{[i]}\right)\right), \tag{70}$$

for T-exchange, and

$$\Delta = \beta_{m_0} \left[\left(E_{\boldsymbol{\lambda}_{m_{\ell+1}}}(q^{[j]}) - E_{\boldsymbol{\lambda}_{m_{\ell+1}}}(q^{[i]}) \right) - \left(E_{\boldsymbol{\lambda}_{m_\ell}}(q^{[j]}) - E_{\boldsymbol{\lambda}_{m_\ell}}(q^{[i]}) \right) \right] , \qquad (71)$$

for $\lambda^{(\ell)}$-exchange (for one of $\ell = 1, \cdots, L$). Here, $q^{[i]}$ and $q^{[j]}$ stand for configuration variables for replicas i and j, respectively, before the replica exchange.

We now consider the *multidimensional simulated tempering* (MST) which realizes a random walk both in temperature T and in parameters $\boldsymbol{\lambda}$ [152, 153, 154]. The entire parameter set $\boldsymbol{\Lambda} = (T, \boldsymbol{\lambda}) \equiv (T, \lambda^{(1)}, \cdots, \lambda^{(L)})$ become dynamical variables and both the configuration and the parameter set are updated during the simulation with a weight factor:

$$W_{\mathrm{MST}}(\boldsymbol{\Lambda}) \equiv \exp \left(-\beta E_{\boldsymbol{\lambda}} + f(\boldsymbol{\Lambda}) \right) , \qquad (72)$$

where the function $f(\boldsymbol{\Lambda}) = f(T, \boldsymbol{\lambda})$ is chosen so that the probability distribution of $\boldsymbol{\Lambda}$ is flat:

$$P_{\mathrm{MST}}(\boldsymbol{\Lambda}) \propto \int dE_0 dV_1 \cdots dV_L \; n(E_0, V_1, \cdots, V_L) \; \exp \left(-\beta E_{\boldsymbol{\lambda}} + f(\boldsymbol{\Lambda}) \right) \equiv \text{constant} . \quad (73)$$

This means that $f(\boldsymbol{\Lambda})$ is the dimensionless ("Helmholtz") free energy:

$$\exp \left(-f(\boldsymbol{\Lambda}) \right) = \int dE_0 dV_1 \cdots dV_L \; n(E_0, V_1, \cdots, V_L) \; \exp(-\beta E_{\boldsymbol{\lambda}}) . \qquad (74)$$

In the numerical work we discretize the parameter set $\boldsymbol{\Lambda}$ in $M(= M_0 \times M_1 \times \cdots \times M_L)$ different values: $\boldsymbol{\Lambda}_m \equiv (T_{m_0}, \boldsymbol{\lambda}_m) \equiv (T_{m_0}, \lambda_{m_1}^{(1)}, \cdots, \lambda_{m_L}^{(L)})$, where $m_0 = 1, \cdots, M_0, m_\ell = 1, \cdots, M_\ell$ ($\ell = 1, \cdots, L$). Without loss of generality we can order the parameters so that $T_1 < T_2 < \cdots < T_{M_0}$ and $\lambda_1^{(\ell)} < \lambda_2^{(\ell)} < \cdots < \lambda_{M_\ell}^{(\ell)}$ (for each $\ell = 1, \cdots, L$). The free energy $f(\boldsymbol{\Lambda}_m)$ is now written as $f_{m_0, m_1, \cdots, m_L} = f(T_{m_0}, \lambda_{m_1}^{(1)}, \cdots, \lambda_{m_L}^{(L)})$.

Once the initial configuration and the initial parameter set are chosen, the multidimensional ST is realized by alternately performing the following two steps:

1. A "canonical" MC or MD simulation at the fixed parameter set $\boldsymbol{\Lambda}_m = (T_{m_0}, \boldsymbol{\lambda}_m) = (T_{m_0}, \lambda_{m_1}^{(1)}, \cdots, \lambda_{m_L}^{(L)})$ is carried out for a certain steps with the weight factor $\exp(-\beta_{m_0} E_{\boldsymbol{\lambda}_m})$ (for fixed $\boldsymbol{\Lambda}_m$, $f(\boldsymbol{\Lambda}_m)$ in Eq. (72) is a constant and does not contribute).

2. We update the parameter set $\boldsymbol{\Lambda}_m$ to a new parameter set $\boldsymbol{\Lambda}_{m\pm1}$ in which one of the parameters in $\boldsymbol{\Lambda}_m$ is changed to a neighboring value with the configuration and the other parameters fixed. The transition probability of this parameter updating process is given by the following Metropolis criterion:

$$w(\boldsymbol{\Lambda}_m \to \boldsymbol{\Lambda}_{m\pm1}) = \min \left(1, \frac{W_{\mathrm{MST}}(\boldsymbol{\Lambda}_{m\pm1})}{W_{\mathrm{MST}}(\boldsymbol{\Lambda}_m)} \right) = \min \left(1, \exp \left(-\Delta \right) \right) . \qquad (75)$$

Here, there are two possibilities for $\boldsymbol{\Lambda}_{m\pm1}$, namely, T-update and $\lambda^{(\ell)}$-update. For T-update, we have $\boldsymbol{\Lambda}_{m\pm1} = (T_{m_0\pm1}, \boldsymbol{\lambda}_m)$ with

$$\Delta = (\beta_{m_0\pm1} - \beta_{m_0}) E_{\boldsymbol{\lambda}_m} - (f_{m_0\pm1, m_1, \cdots, m_L} - f_{m_0, m_1, \cdots, m_L}) . \qquad (76)$$

For $\lambda^{(\ell)}$-update (for one of $\ell = 1, \cdots, L$), we have $\boldsymbol{\Lambda}_{m\pm1} = (T_{m_0}, \boldsymbol{\lambda}_{m_\ell\pm1})$ with

$$\Delta = \beta_{m_0}(E_{\boldsymbol{\lambda}_{m_\ell\pm1}} - E_{\boldsymbol{\lambda}_{m_\ell}}) - (f_{m_0, \cdots, m_\ell\pm1, \cdots} - f_{m_0, \cdots, m_\ell, \cdots}) , \qquad (77)$$

where $\boldsymbol{\lambda}_{m_\ell\pm1} = (\cdots, \lambda_{m_{\ell-1}}^{(\ell-1)}, \lambda_{m_\ell\pm1}^{(\ell)}, \lambda_{m_{\ell+1}}^{(\ell+1)}, \cdots)$ and $\boldsymbol{\lambda}_{m_\ell} = (\cdots, \lambda_{m_{\ell-1}}^{(\ell-1)}, \lambda_{m_\ell}^{(\ell)}, \lambda_{m_{\ell+1}}^{(\ell+1)}, \cdots)$.

We now describe the *multidimensional multicanonical algorithm* (MMUCA) which realizes a random walk in the $(L+1)$-dimensional space of $E_0(x)$ and $V_\ell(x)$ ($\ell = 1, \cdots, L$).

In the multidimensional MUCA ensemble, each state is weighted by the MUCA weight factor $W_{\text{MMUCA}}(E_0, V_1, \cdots, V_L)$ so that a uniform energy distribution of $E_0, V_1, \cdots,$ and V_L may be obtained:

$$P_{\text{MMUCA}}(E_0, V_1, \cdots, V_L) \propto n(E_0, V_1, \cdots, V_L)W_{\text{MMUCA}}(E_0, V_1, \cdots, V_L) \equiv \text{constant} , \quad (78)$$

where $n(E_0, V_1, \cdots, V_L)$ is the multidimensional density of states. From this equation, we obtain

$$W_{\text{MMUCA}}(E_0, V_1, \cdots, V_L) \equiv \exp\left(-\beta_a E_{\text{MMUCA}}(E_0, V_1, \cdots, V_L)\right) \propto \frac{1}{n(E_0, V_1, \cdots, V_L)} , \tag{79}$$

where we have introduced an arbitrary reference temperature, $T_a = 1/k_{\text{B}}\beta_a$, and wrote the weight factor in the Boltzmann-like form. Here, the "*multicanonical potential energy*" is defined by

$$E_{\text{MMUCA}}(E_0, V_1, \cdots, V_L; T_a) \equiv k_{\text{B}}T_a \ln n(E_0, V_1, \cdots, V_L) . \tag{80}$$

The multidimensional MUCA MC simulation can be performed with the following Metropolis transition probability from state x with energy $E_{\boldsymbol{\lambda}} = E_0 + \sum_{\ell=1}^{L} \lambda^{(\ell)}V_\ell$ to state x' with energy $E_{\boldsymbol{\lambda}}' = E_0' + \sum_{\ell=1}^{L} \lambda^{(\ell)}V_\ell'$:

$$w(x \to x') = \min\left(1, \frac{W_{\text{MMUCA}}(E_0', V_1', \cdots, V_L')}{W_{\text{MMUCA}}(E_0, V_1, \cdots, V_L)}\right) = \min\left(1, \frac{n(E_0, V_1, \cdots, V_L)}{n(E_0', V_1', \cdots, V_L')}\right) . \tag{81}$$

A MD algorithm in the multidimensional MUCA ensemble also naturally follows from Eq. (79), in which a regular constant temperature MD simulation (with $T = T_a$) is performed by replacing the total potential energy $E_{\boldsymbol{\lambda}}$ by the multicanonical potential energy E_{MMUCA} in Eq. (12):

$$\dot{\boldsymbol{p}}_k = -\frac{\partial E_{\text{MMUCA}}(E_0, V_1, \cdots, V_L; T_a)}{\partial \boldsymbol{q}_k} - \frac{\dot{s}}{s} \boldsymbol{p}_k . \tag{82}$$

We remark that the random walk in E_0 and in V_ℓ for the MUCA simulation corresponds to that in β and in $\beta\lambda^{(\ell)}$ for the ST simulation:

$$\begin{cases} E_0 & \longleftrightarrow \beta , \\ V_\ell & \longleftrightarrow \beta\lambda^{(\ell)} , \quad (\ell = 1, \cdots, L) . \end{cases} \tag{83}$$

They are in conjugate relation.

3.2 Weight Factor Determinations for Multidimensional ST and MUCA

Among the three multidimensional generalized-ensemble algorithms described above, only MREM can be performed without much preparation because the weight factor for MREM is just a product of regular Boltzmann-like factors. On the other hand, we do not know the MST and MMUCA weight factors *a priori* and need to estimate them. As a simple

method for these weight factor determinations, we can generalize the REST and REMUCA presented in the previous subsections to multidimensions.

Suppose we have made a single run of a short MREM simulation with $M(= M_0 \times M_1 \times \cdots \times M_L)$ replicas that correspond to M different parameter sets $\mathbf{\Lambda}_m$ ($m = 1, \cdots, M$). Let $N_{m_0, m_1, \cdots, m_L}(E_0, V_1, \cdots, V_L)$ and $n_{m_0, m_1, \cdots, m_L}$ be respectively the $(L+1)$-dimensional potential-energy histogram and the total number of samples obtained for the m-th parameter set $\mathbf{\Lambda}_m = (T_{m_0}, \lambda_{m_1}^{(1)}, \cdots, \lambda_{m_L}^{(L)})$. The generalized WHAM equations are then given by

$$
n(E_0, V_1, \cdots, V_L) = \frac{\displaystyle\sum_{m_0, m_1, \cdots, m_L} N_{m_0, m_1, \cdots, m_L}(E_0, V_1, \cdots, V_L)}{\displaystyle\sum_{m_0, m_1, \cdots, m_L} n_{m_0, m_1, \cdots, m_L} \exp\left(f_{m_0, m_1, \cdots, m_L} - \beta_{m_0} E_{\boldsymbol{\lambda}_m}\right)} \;,
\tag{84}
$$

and

$$
\exp(-f_{m_0, m_1, \cdots, m_L}) = \sum_{E_0, V_1, \cdots, V_L} n(E_0, V_1, \cdots, V_L) \exp\left(-\beta_{m_0} E_{\boldsymbol{\lambda}_m}\right) \;.
\tag{85}
$$

The density of states $n(E_0, V_1, \cdots, V_L)$ (which is inversely proportional to the MMUCA weight factor) and the dimensionless free energy $f_{m_0, m_1, \cdots, m_L}$ (which is the MST parameter) are obtained by solving Eqs. (84) and (85) self-consistently by iteration.

3.3 Expectation Values of Physical Quantities

We now present the equations to calculate ensemble averages of physical quantities with any temperature T and any parameter $\boldsymbol{\lambda}$ values.

After a long production run of MREM and MST simulations, the canonical expectation value of a physical quantity A with the parameter values $\mathbf{\Lambda}_m$ ($m = 1, \cdots, M$), where $\mathbf{\Lambda}_m \equiv (T_{m_0}, \boldsymbol{\lambda}_m) \equiv (T_{m_0}, \lambda_{m_1}^{(1)}, \cdots, \lambda_{m_L}^{(L)})$ with $m_0 = 1, \cdots, M_0, m_\ell = 1, \cdots, M_\ell$ ($\ell = 1, \cdots, L$), and $M(= M_0 \times M_1 \times \cdots \times M_L)$, can be calculated by the usual arithmetic mean:

$$
< A >_{T_{m_0}, \boldsymbol{\lambda}_m} = \frac{1}{n_m} \sum_{k=1}^{n_m} A\left(x_m(k)\right) \;,
\tag{86}
$$

where $x_m(k)$ ($k = 1, \cdots, n_m$) are the configurations obtained with the parameter values $\mathbf{\Lambda}_m$ ($m = 1, \cdots, M$), and n_m is the total number of measurements made with these parameter values. The expectation values of A at any intermediate T ($= 1/k_\mathrm{B}\beta$) and any $\boldsymbol{\lambda}$ can also be obtained from

$$
< A >_{T, \boldsymbol{\lambda}} = \frac{\displaystyle\sum_{E_0, V_1, \cdots, V_L} A(E_0, V_1, \cdots, V_L) n(E_0, V_1, \cdots, V_L) \exp\left(-\beta E_{\boldsymbol{\lambda}}\right)}{\displaystyle\sum_{E_0, V_1, \cdots, V_L} n(E_0, V_1, \cdots, V_L) \exp\left(-\beta E_{\boldsymbol{\lambda}}\right)} \;,
\tag{87}
$$

where the density of states $n(E_0, V_1, \cdots, V_L)$ is obtained from the multiple-histogram reweighting techniques. Namely, from the MREM or MST simulation, we first obtain the histogram $N_{m_0, m_1, \cdots, m_L}(E_0, V_1, \cdots, V_L)$ and the total number of samples $n_{m_0, m_1, \cdots, m_L}$ in Eq. (84). The density of states $n(E_0, V_1, \cdots, V_L)$ and the dimensionless free energy $f_{m_0, m_1, \cdots, m_L}$ are then obtained by solving Eqs. (84) and (85) self-consistently by iteration. Substituting the obtained density of states $n(E_0, V_1, \cdots, V_L)$ into Eq. (87), one can calculate the ensemble average of the physical quantity A at any T and any $\boldsymbol{\lambda}$.

Moreover, the ensemble average of the physical quantity A (including those that cannot be expressed as functions of E_0 and V_ℓ ($\ell = 1, \cdots, L$)) can be obtained from the "trajectory" of configurations of the production run [153]. Namely, we first obtain $f_{m_0, m_1, \cdots, m_L}$ for each ($m_0 = 1, \cdots, M_0, m_1 = 1, \cdots, M_1, \cdots, m_L = 1, \cdots, M_L$) by solving Eqs. (84) and (85) self-consistently, and then we have

$$
< A >_{T, \boldsymbol{\lambda}} = \frac{\displaystyle\sum_{m_0=1}^{M_0} \cdots \sum_{m_L=1}^{M_L} \sum_{x_m} A(x_m) \dfrac{\exp\left(-\beta E_{\boldsymbol{\lambda}}(x_m)\right)}{\displaystyle\sum_{n_0=1}^{M_0} \cdots \sum_{n_L=1}^{M_L} n_{n_0, \cdots, n_L} \exp\left(f_{n_0, \cdots, n_L} - \beta_{n_0} E_{\boldsymbol{\lambda}_n}(x_m)\right)}}{\displaystyle\sum_{m_0=1}^{M_0} \cdots \sum_{m_L=1}^{M_L} \sum_{x_m} \dfrac{\exp\left(-\beta E_{\boldsymbol{\lambda}}(x_m)\right)}{\displaystyle\sum_{n_0=1}^{M_0} \cdots \sum_{n_L=1}^{M_L} n_{n_0, \cdots, n_L} \exp\left(f_{n_0, \cdots, n_L} - \beta_{n_0} E_{\boldsymbol{\lambda}_n}(x_m)\right)}} ,
\tag{88}
$$

where x_m are the configurations obtained at $\boldsymbol{\Lambda}_m = (T_{m_0}, \boldsymbol{\lambda}_m) = (T_{m_0}, \lambda_{m_1}^{(1)}, \cdots, \lambda_{m_L}^{(L)})$. Here, the trajectories x_m are stored for each $\boldsymbol{\Lambda}_m$ separately.

For the MMUCA simulation with the weight factor $W_{\text{MMUCA}}(E_0, \cdots, V_L)$, the expectation values of A at any T ($= 1/k_B\beta$) and any $\boldsymbol{\lambda}$ can also be obtained from Eq. (87) by the single-histogram reweighting techniques as follows. Let $N_{\text{MMUCA}}(E_0, V_1, \cdots, V_L)$ be the histogram of the distribution of $E_0, V_1, \cdots, V_L$, $P_{\text{MMUCA}}(E_0, V_1, \cdots, V_L)$, obtained by the production run. The best estimate of the density of states $n(E_0, V_1, \cdots, V_L)$ is then given by

$$
n(E_0, V_1, \cdots, V_L) = \frac{N_{\text{MMUCA}}(E_0, V_1, \cdots, V_L)}{W_{\text{MMUCA}}(E_0, \cdots, V_L)} .
\tag{89}
$$

Moreover, the ensemble average of the physical quantity A (including those that cannot be expressed as a function of E_0 and V_ℓ ($\ell = 1, \cdots, L$)) can be obtained as long as one stores the "trajectory" of configurations x_k from the production run. We have

$$
< A >_{T, \boldsymbol{\lambda}} = \frac{\displaystyle\sum_{k=1}^{n_s} A(x_k) W_{\text{MMUCA}}^{-1}(E_0(x_k), \cdots, V_L(x_k)) \exp\left(-\beta E_{\boldsymbol{\lambda}}(x_k)\right)}{\displaystyle\sum_{k=1}^{n_s} W_{\text{MMUCA}}^{-1}(E_0(x_k), \cdots, V_L(x_k)) \exp\left(-\beta E_{\boldsymbol{\lambda}}(x_k)\right)} .
\tag{90}
$$

Here, x_k is the configuration at the k-th MC (or MD) step and n_s is the total number of configurations stored.

3.4 Multidimensional Generalized-Ensemble Algorithms for the Isobaric-Isothermal Ensemble

As examples of the multidimensional formulations in the previous subsections, we present the generalized-ensemble algorithms for the isobaric-isothermal ensemble (or, the NPT ensemble) [155]. Let us consider a physical system that consists of N atoms and that is in a box of a finite volume $\mathcal{V}$. The states of the system are specified by coordinates $q \equiv \{\boldsymbol{q}_1, \boldsymbol{q}_2, \cdots, \boldsymbol{q}_N\}$ and momenta $p \equiv \{\boldsymbol{p}_1, \boldsymbol{p}_2, \cdots, \boldsymbol{p}_N\}$ of the atoms and volume $\mathcal{V}$ of the box. The potential energy $E(q, \mathcal{V})$ for the system is a function of q and $\mathcal{V}$.

In the isobaric-isothermal ensemble [157, 158, 163, 170] the probability distribution $P_{\mathrm{NPT}}(E, \mathcal{V}; T, \mathcal{P})$ for potential energy E and volume $\mathcal{V}$ at temperature T and pressure $\mathcal{P}$ is given by

$$P_{\mathrm{NPT}}(E, \mathcal{V}; T, \mathcal{P}) \propto n(E, \mathcal{V}) W_{\mathrm{NPT}}(E, \mathcal{V}; T, \mathcal{P}) = n(E, \mathcal{V}) \mathrm{e}^{-\beta \mathcal{H}} \ . \tag{91}$$

Here, the density of states $n(E, \mathcal{V})$ is given as a function of both E and $\mathcal{V}$, and $\mathcal{H}$ is the "enthalpy" (without the kinetic energy contributions):

$$\mathcal{H} = E + \mathcal{P} \mathcal{V} \ . \tag{92}$$

This weight factor produces an isobaric-isothermal ensemble at constant temperature (T) and constant pressure $(\mathcal{P})$. Note that this is a special case of the general formulations in Eq. (65) with $L = 1$, $E_0 = E$, $V_1 = \mathcal{V}$, and $\lambda^{(1)} = \mathcal{P}$.

In order to perform the isobaric-isothermal MC simulation [170], we perform Metropolis sampling on the scaled coordinates $\sigma = \{\boldsymbol{\sigma}_1, \boldsymbol{\sigma}_2, \cdots, \boldsymbol{\sigma}_N\}$ where $\boldsymbol{\sigma}_k = \mathcal{V}^{-1/3} \boldsymbol{q}_k$ ($k = 1, 2, \cdots, N$) ($\boldsymbol{q}_k$ are the real coordinates) and the volume $\mathcal{V}$ (here, the particles are placed in a cubic box of a side of size $\mathcal{V}^{-1/3}$). The trial moves from state x with the scaled coordinates σ with volume $\mathcal{V}$ to state x' with the scaled coordinate σ' and volume $\mathcal{V}'$ are generated by uniform random numbers. The enthalpy is accordingly changed from $\mathcal{H}(E(\sigma, \mathcal{V}), \mathcal{V})$ to $\mathcal{H}'(E(\sigma', \mathcal{V}'), \mathcal{V}')$ by these trial moves. The trial moves will be accepted with the following Metropolis criterion:

$$w(x \to x') = \min\left(1, \exp[-\beta\{\mathcal{H}' - \mathcal{H} - N k_{\mathrm{B}} T \ln(\mathcal{V}'/\mathcal{V})\}]\right) \ , \tag{93}$$

where N is the total number of atoms in the system.

As for the MD method in this ensemble, we just present the Nosé-Andersen algorithm [157, 158, 163]. The equations of motion in Eqs. (11)–(14) are now generalized as follows:

$$\dot{\boldsymbol{q}}_k = \frac{\boldsymbol{p}_k}{m_k} + \frac{\dot{\mathcal{V}}}{3\mathcal{V}} \boldsymbol{q}_k \ , \tag{94}$$

$$\dot{\boldsymbol{p}}_k = -\frac{\partial \mathcal{H}}{\partial \boldsymbol{q}_k} - \left(\frac{\dot{s}}{s} + \frac{\dot{\mathcal{V}}}{3\mathcal{V}}\right) \boldsymbol{p}_k \tag{95}$$

$$= \boldsymbol{f}_k - \left(\frac{\dot{s}}{s} + \frac{\dot{\mathcal{V}}}{3\mathcal{V}}\right) \boldsymbol{p}_k \ , \tag{96}$$

$$\dot{s} = s \frac{P_s}{Q} \ , \tag{97}$$

$$\dot{P}_s = \sum_{i=1}^{N} \frac{\boldsymbol{p}_i^2}{m_i} - 3N k_{\mathrm{B}} T = 3N k_{\mathrm{B}} \left(T(t) - T\right) \ , \tag{98}$$

$$\dot{\mathcal{V}} = s \frac{P_{\mathcal{V}}}{\mathcal{M}} \ , \tag{99}$$

$$\dot{P}_{\mathcal{V}} = s \left[\frac{1}{3\mathcal{V}} \left(\sum_{i=1}^{N} \frac{\boldsymbol{p}_i^2}{m_i} - \sum_{i=1}^{N} \boldsymbol{q}_i \cdot \frac{\partial \mathcal{H}}{\partial \boldsymbol{q}_i}\right) - \frac{\partial \mathcal{H}}{\partial \mathcal{V}}\right] \tag{100}$$

$$= s \left(\mathcal{P}(t) - \mathcal{P}\right) \ , \tag{101}$$

where $\mathcal{M}$ is the artificial mass associated with the volume, $P_\mathcal{V}$ is the conjugate momentum for the volume, and the "instantaneous pressure" $\mathcal{P}(t)$ is defined by

$$\mathcal{P}(t) = \frac{1}{3\mathcal{V}}\left(\sum_{i=1}^{N}\frac{\boldsymbol{p}_i(t)^2}{m_i} + \sum_{i=1}^{N}\boldsymbol{q}_i(t)\cdot\boldsymbol{f}_i(t)\right) - \frac{\partial E}{\partial\mathcal{V}}(t) . \tag{102}$$

In REM simulations for the NPT ensemble, we prepare a system that consists of $M_T \times M_\mathcal{P}$ non-interacting replicas of the original system, where M_T and $M_\mathcal{P}$ are the number of temperature and pressure values used in the simulation, respectively. The replicas are specified by labels i ($i = 1, 2, \cdots, M_T \times M_\mathcal{P}$), temperature by m_0 ($m_0 = 1, 2, \cdots, M_T$) and pressure by m_1 ($m_1 = 1, 2, \cdots, M_\mathcal{P}$).

To perform REM simulations, we carry out the following two steps alternately: (1) perform a usual constant NPT MC or MD simulation in each replica at assigned temperature and pressure and (2) try to exchange the replicas. If the temperature (specified by m_0 and n_0) or pressure (specified by m_1 and n_1) between the replicas is exchanged in Step 2, the transition probability from $X \equiv \{\cdots, (\sigma^{[i]}, \mathcal{V}^{[i]}; T_{m_0}, \mathcal{P}_{m_1}), \cdots, (\sigma^{[j]}, \mathcal{V}^{[j]}; T_{n_0}, \mathcal{P}_{n_1}), \cdots\}$ to $X' \equiv \{\cdots, (\sigma^{[i]}, \mathcal{V}^{[i]}; T_{n_0}, \mathcal{P}_{n_1}), \cdots, (\sigma^{[j]}, \mathcal{V}^{[j]}; T_{m_0}, \mathcal{P}_{m_1}), \cdots\}$ at the trial is given by [118, 11]

$$w_{\text{REM}}(X \to X') = \min\left[1, \exp(-\Delta_{\text{REM}})\right], \tag{103}$$

where

$$\Delta_{\text{REM}} = (\beta_{m_0} - \beta_{n_0})\left[E(\sigma^{[j]}, \mathcal{V}^{[j]}) - E(\sigma^{[i]}, \mathcal{V}^{[i]})\right] + (\beta_{m_0}\mathcal{P}_{m_1} - \beta_{n_0}\mathcal{P}_{n_1})\left(\mathcal{V}^{[j]} - \mathcal{V}^{[i]}\right). \tag{104}$$

In ST simulations for the NPT ensemble, we introduce a function $f(T, \mathcal{P})$ and use a weight factor $W_{\text{ST}}(E, \mathcal{V}; T, \mathcal{P}) \equiv \exp[-\beta(E + \mathcal{P}\mathcal{V}) + f(T, \mathcal{P})]$ so that the distribution function $P_{\text{ST}}(T, \mathcal{P})$ of T and $\mathcal{P}$ may be uniform:

$$P_{\text{ST}}(T, \mathcal{P}) \propto \int_0^\infty d\mathcal{V} \int_\mathcal{V} dq\, W_{\text{ST}}[E(q, \mathcal{V}), \mathcal{V}; T, \mathcal{P}] = \text{constant} . \tag{105}$$

From Eq. (105), it is found that $f(T, \mathcal{P})$ is formally given by

$$f(T, \mathcal{P}) = -\ln\left\{\int_0^\infty d\mathcal{V} \int_\mathcal{V} dq \exp\left[-\beta\left(E(q, \mathcal{V}) + \mathcal{P}\mathcal{V}\right)\right]\right\}, \tag{106}$$

and this function is the dimensionless Gibbs free energy except for a constant.

To perform ST simulations, we again discretize temperature and pressure into $M_0 \times M_1$ set of values $(T_{m_0}, \mathcal{P}_{m_1})$ ($m_0 = 1, \cdots, M_0$, $m_1 = 1, \cdots, M_1$). We carry out the following two steps alternately: (1) perform a usual constant NPT MC or MD simulation and (2) try to update the temperature or pressure. In Step 2 the transition probability from the state $X \equiv \{\sigma, \mathcal{V}; T_{m_0}, \mathcal{P}_{m_1}\}$ to the state $X' \equiv \{\sigma, \mathcal{V}; T_{n_0}, \mathcal{P}_{n_1}\}$ is given by

$$w_{\text{ST}}(X \to X') = \min\left[1, \exp(-\Delta_{\text{ST}})\right], \tag{107}$$

where

$$\Delta_{\text{ST}} = (\beta_{n_0} - \beta_{m_0})E(\sigma, \mathcal{V}) + (\beta_{n_0}\mathcal{P}_{n_1} - \beta_{m_0}\mathcal{P}_{m_1})\mathcal{V} - (f_{n_0,n_1} - f_{m_0,m_1}) . \tag{108}$$

We remark that when we perform MD simulations with REM and ST, the momenta should be rescaled if the replicas are exchanged for the temperature in REM and the temperature is updated in ST as shown above in the previous subsections.

From the production run of REM or ST simulations in the NPT ensemble, we can calculate isobaric-isothermal averages of a physical quantity A at $(T_{m_0}, \mathcal{P}_{m_1})$ $(m_0 = 1, \cdots, M_0,\ m_1 = 1, \cdots, M_1)$ by the usual arithmetic mean:

$$< A >_{T_{m_0}, \mathcal{P}_{m_1}} = \frac{1}{n_m} \sum_{k=1}^{n_m} A\left(x_m(k)\right) , \qquad (109)$$

where $x_m(k)$ $(k = 1, \cdots, n_m)$ are the configurations obtained with the parameter values $(T_{m_0}, \mathcal{P}_{m_1})$ and n_m is the total number of measurements made with these parameter values. The expectation values of A at any intermediate temperature T $(= 1/k_B\beta)$ and any intermediate pressure $\mathcal{P}$ can also be obtained from

$$< A >_{T,\mathcal{P}} = \frac{\displaystyle\sum_{E,\mathcal{V}} A(E, \mathcal{V}) n(E, \mathcal{V}) \exp\left(-\beta(E + \mathcal{P}\mathcal{V})\right)}{\displaystyle\sum_{E,\mathcal{V}} n(E, \mathcal{V}) \exp\left(-\beta(E + \mathcal{P}\mathcal{V})\right)} , \qquad (110)$$

where the density of states $n(E, \mathcal{V})$ is obtained from the multiple-histogram reweighting techniques. Namely, from the REM or ST simulation, we first obtain the histogram $N_{m_0,m_1}(E, \mathcal{V})$ and the total number of samples n_{m_0,m_1}. The density of states $n(E, \mathcal{V})$ and the dimensionless free energy f_{m_0,m_1} are then obtained by solving the following equations self-consistently by iteration (see Eqs. (84) and (85) above):

$$n(E, \mathcal{V}) = \frac{\displaystyle\sum_{m_0,m_1} N_{m_0,m_1}(E, \mathcal{V})}{\displaystyle\sum_{m_0,m_1} n_{m_0,m_1} \exp\left(f_{m_0,m_1} - \beta_{m_0}(E + \mathcal{P}_{m_1}\mathcal{V})\right)} , \qquad (111)$$

and

$$\exp(-f_{m_0,m_1}) = \sum_{E,\mathcal{V}} n(E, \mathcal{V}) \exp\left(-\beta_{m_0}(E + \mathcal{P}_{m_1}\mathcal{V})\right) . \qquad (112)$$

Substituting the obtained density of states $n(E, \mathcal{V})$ into Eq. (110), one can calculate the ensemble average of the physical quantity A at any T and any $\mathcal{P}$.

We now introduce the multicanonical algorithm into the isobaric-isothermal ensemble and refer to this generalized-ensemble algorithm as the *multibaric-multithermal algorithm* (MUBATH) [70]–[73]. The molecular simulations in this generalized ensemble perform random walks both in the potential energy space and in the volume space.

In the MUBATH ensemble, each state is sampled by the MUBATH weight factor $W_{\text{mbt}}(E, \mathcal{V}) \equiv \exp\{-\beta_a \mathcal{H}_{\text{mbt}}(E, \mathcal{V})\}$ ($\mathcal{H}_{\text{mbt}}$ is referred to as the multibaric-multithermal enthalpy) so that a uniform distribution in both potential energy E and volume $\mathcal{V}$ is obtained [70]:

$$P_{\text{mbt}}(E, \mathcal{V}) \propto n(E, \mathcal{V}) W_{\text{mbt}}(E, \mathcal{V}) = n(E, \mathcal{V}) \exp\{-\beta_a \mathcal{H}_{\text{mbt}}(E, \mathcal{V})\} \equiv \text{constant} , \quad (113)$$

where we have chosen an arbitrary reference temperature, $T_a = 1/k_B\beta_a$.

The MUBATH MC simulation can be performed by replacing $\mathcal{H}$ by $\mathcal{H}_{\text{mbt}}$ in Eq. (93):

$$w(x \to x') = \min\left(1, \exp[-\beta_a\{\mathcal{H}'_{\text{mbt}} - \mathcal{H}_{\text{mbt}} - Nk_BT_a \ln(\mathcal{V}'/\mathcal{V})\}]\right) , \qquad (114)$$

In order to perform the MUBATH MD simulation, we just solve the above equations of motion (Eqs. (94)–(101)) for the regular isobaric-isothermal ensemble (with arbitrary

reference temperature $T = T_a$), where the enthalpy $\mathcal{H}$ is replaced by the multibaric-multithermal enthalpy $\mathcal{H}_{\mathrm{mbt}}$ in Eqs. (95) and (100) [72].

In order to calculate the isobaric-isothermal-ensemble averages, we employ the single-histogram reweighting techniques [17]. The expectation value of a physical quantity A at any T and any $\mathcal{P}$ is obtained by substituting the following density of states into Eq. (110):

$$n(E, \mathcal{V}) = \frac{N_{\mathrm{mbt}}(E, \mathcal{V})}{W_{\mathrm{mbt}}(E, \mathcal{V})} \ , \tag{115}$$

where $N_{\mathrm{mbt}}(E, \mathcal{V})$ is the histogram of the probability distribution $P_{\mathrm{mbt}}(E, \mathcal{V})$ of potential energy and volume that was obtained by the MUBATH production run.

4   EXAMPLES OF SIMULATION RESULTS

We tested the effectiveness of the generalized-ensemble algorithms by using a system of a 17-residue fragment of ribonuclease T_1 [171, 108]. It is known by experiments that this peptide fragment forms α-helical conformations [171]. We have performed a two-dimensional REM simulation and a two-dimensional ST simulation. In these simulations, we used the following energy function:

$$E_\lambda = E_0 + \lambda E_{\mathrm{SOL}} \ , \tag{116}$$

where we set $L = 1, V_1 = E_{\mathrm{SOL}}$, and $\lambda^{(1)} = \lambda$ in Eq. (65). Here, E_0 is the potential energy of the solute and E_{SOL} is the solvation free energy. The parameters in the conformational energy as well as the molecular geometry were taken from ECEPP/2 [172, 173, 174].

The solvation term E_{SOL} is given by the sum of terms that are proportional to the solvent-accessible surface area of heavy atoms of the solute [175]. For the calculations of solvent-accessible surface area, we used the computer code NSOL [176].

The computer code KONF90 [7, 8] was modified in order to accommodate the generalized-ensemble algorithms. The simulations were started from randomly generated conformations. We prepared eight temperatures ($M_0 = 8$) which are distributed exponentially between $T_1 = 300$ K and $T_{M_0} = 700$ K (i.e., 300.00, 338.60, 382.17, 431.36, 486.85, 549.49, 620.20, and 700.00 K) and four equally-spaced λ values ($M_1 = 4$) ranging from 0 to 1 (i.e., $\lambda_1 = 0, \lambda_2 = 1/3, \lambda_3 = 2/3$, and $\lambda_4 = 1$) in the two-dimensional REM simulation and the two-dimensional ST simulation. Simulations with $\lambda = 0$ (i.e., $E_\lambda = E_0$) and with $\lambda = 1$ (i.e., $E_\lambda = E_0 + E_{\mathrm{SOL}}$) correspond to those in gas phase and in aqueous solution, respectively.

We first present the results of the two-dimensional REM simulation. We used 32 replicas with the eight temperature values and the four λ values given above. Before taking the data, we made the two-dimensional REM simulation of 100000 MC sweeps with each replica for thermalization. We then performed the two-dimensional REM simulation of 1000000 MC sweeps for each replica to determine the weight factor for the two-dimensional ST simulation. At every 20 MC sweeps, either T-exchange or λ-exchange was tried (the choice of T or λ was made randomly). In each case, either set of pairs of replicas $((1,2),...,(M{-}1,M))$ or $((2,3),...,(M,1))$ was also chosen randomly, where M is M_0 and M_1 for T-exchange and λ-exchange, respectively.

In Fig. 1 we show the time series of labels of T_{m_0} (i.e., m_0) and λ_{m_1} (i.e., m_1) for one of the replicas. The replica realized a random walk not only in temperature space but also
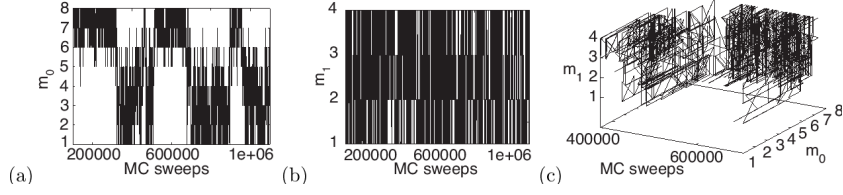
25

Figure 1: Time series of the labels of T_{m_0}, m_0, (a) and λ_{m_1}, m_1, (b) as functions of MC sweeps, and that of both m_0 and m_1 for the region from 400000 MC sweeps to 700000 MC sweeps (c). The results were from one of the replicas (Replica 1). In (a) and (b), MC sweeps start at 100000 and end at 1100000 because the first 100000 sweeps have been removed from the consideration for thermalization purpose.

in λ space. The behavior of T and λ for other replicas was also similar (see Ref. [154]). From Fig. 1, one finds that the λ-random walk is more frequent than the T-random walk.
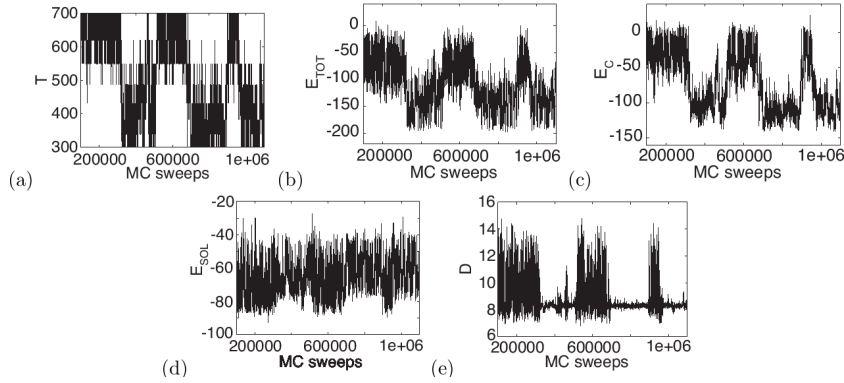
Figure 2: Time series of the temperature T (a), total energy E_{TOT} (b), conformational energy E_{C} (c), solvation free energy E_{SOL} (d), and end-to-end distance D (e) for the same replica as in Fig. 1. The temperature is in K, the energy is in kcal/mol, and the end-to-end distance is in Å.

We also show the time series of temperature T, total energy E_{TOT}, conformational energy E_{C}, solvation free energy E_{SOL}, and end-to-end distance D for the same replica in Fig. 2. From Figs. 2(a) and 2(e), we find that at lower temperatures the end-to-end distance is about 8 Å, which is the length of a fully α-helical conformation and that at higher temperatures it fluctuates much for a range from 7 Å to 14 Å. It suggests that α-helix structures exist at low temperatures and random-coil structures occur at high temperatures. There are transitions from/to α-helix structures to/from random coils during the simulation. It indicates that the REM simulation avoided getting trapped in local-minimum-energy states and sampled a wide conformational space.

The canonical probability distributions of E_{TOT} and E_{SOL} at the 32 conditions obtained from the two-dimensional REM simulation are shown in Fig. 3. For an optimal performance of the REM simulation, there should be enough overlaps between all pairs of neighboring distributions, which will lead to sufficiently uniform and large acceptance ratios of replica exchanges. There are indeed ample overlaps between the neighboring distributions in Fig. 3.
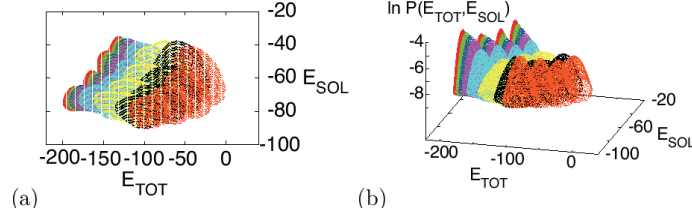
26

Figure 3: Contour curves and histograms of distributions of the total energy E_{TOT} and the solvation free energy E_{SOL} ((a) and (b)) from the two-dimensional REM simulation.

We now use the results of the two-dimensional REM simulation to determine the weight factors for the two-dimensional ST simulation by the multiple-histogram reweighting techniques. Namely, by solving the generalized WHAM equations in Eqs. (84) and (85) with the obtained histograms at the 32 conditions (see Fig. 3), we obtained 32 values of the ST parameters $f_{m_0, m_1}(m_0 = 1, \cdots, 8; m_1 = 1, \cdots, 4)$.

After obtaining the ST weight factor, $W_{ST} = \exp(-\beta_{m_0}(E_{\text{C}} + \lambda_{m_1}E_{\text{SOL}}) + f_{m_0, m_1})$, we carried out the two-dimensional ST simulation of 1000000 MC sweeps for data collection after 100000 MC sweeps for thermalization. At every 20 MC sweeps, either T_{m_0} or λ_{m_1} was respectively updated to $T_{m_0 \pm 1}$ or $\lambda_{m_1 \pm 1}$ (the choice of T or λ update and the choice of ± 1 were made randomly).

We show the average total energy, average conformational energy, average $\lambda \times E_{\text{SOL}}$, and average end-to-end distance in Fig. 4. The results are in good agreement with those of the REM simulation (data not shown).
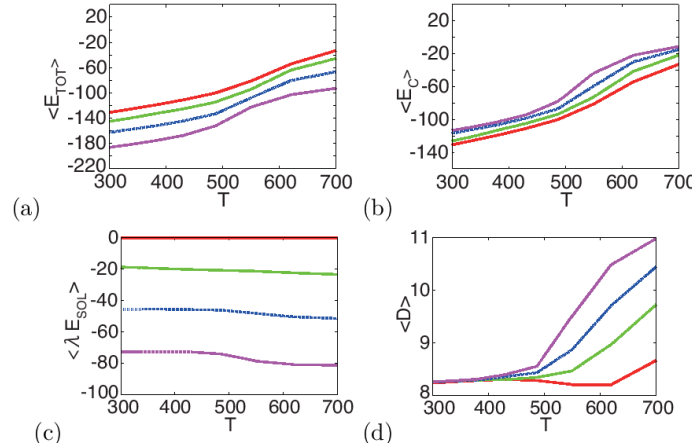
Figure 4: The average total energy (a), average conformational energy (b), average of $\lambda \times E_{\text{SOL}}$ (c), and average end-to-end distance (d) with all the λ values as functions of temperature. The lines colored in red, green, blue, and purple are for λ_1, λ_2, λ_3, and λ_4, respectively. They are in order from above to below in (a) and (c) and from below to above in (b) and (d).

We found that the results of the two-dimensional ST simulation are in complete agreement with those of the two-dimensional REM simulation for the average quantities. The only difference between the two simulations is the number of replicas. In the present

simulation, while the REM simulation used 32 replicas, the ST simulation used only one replica. Hence, we can save much computer power with ST.

A second example of our multidimensional generalized-ensemble simulations is a pressure ST (PST) simulation in the isobaric-isothermal ensemble [155]. This simulation performs a random walk in one-dimensional pressure space. The system that we simulated is ubiquitin in explicit water. This system has been studied by high pressure NMR experiments and known to undergo high-pressure denaturations [177, 178]. Ubiquitin has 76 amino acids and it was placed in a cubic box of 6232 water molecules. Temperature was fixed to be 300 K throughout the simulations, and we prepared 100 values of pressure ranging from 1 bar to 10000 bar. Temperature and pressure were controlled by Hoover-Langevin method [179] and particle mesh Ewald method [180, 181] were employed for electrostatic interactions. The time step was 2.0 fsec. The force field CHARMM22 [182] with CMAP [183, 184] and TIP3P water model [185, 182] were used, and the program package NAMD version 2.7b3 [186] was modified to incorporate the PST algorithm.

We first performed 100 independent conventional isobaric-isothermal simulations of 4 nsec with $T = 300$ K (i.e., $M_0 = 1$) and 100 values of pressure (i.e., $M_1 = 100$). Using the obtained histogram $N_{m_0,m_1}(E, \mathcal{V})$ of potential energy and volume distribution, we obtained the ST parameters f_{m_0,m_1} by solving the WHAM equations in Eqs. (111) and (112). We then performed the PST production of 500 nsec and repeated it 10 times with different seeds for random numbers (so, the total simulation time for the production run is 5.0 μsec).

In Fig. 5 we show the time series of pressure and potential energy during the PST production run.
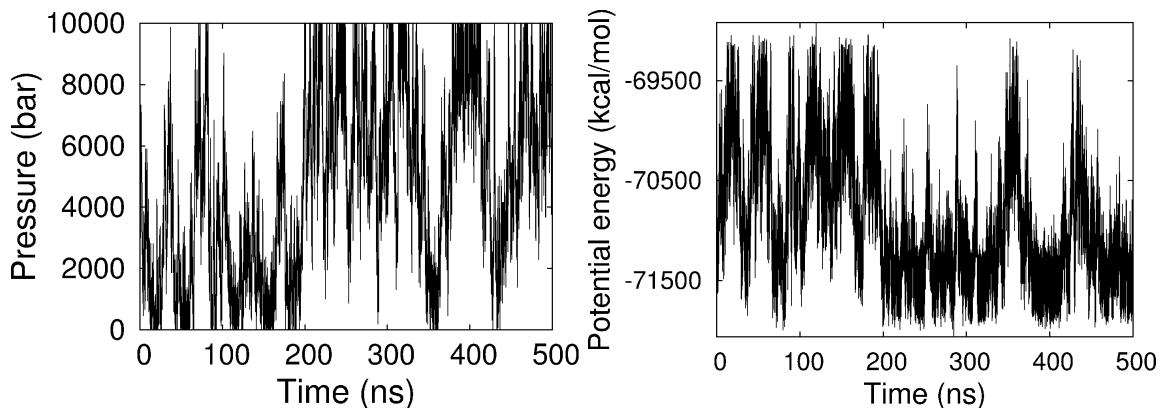

Figure 5: Time series of pressure (left) and potential energy (right) during the PST production run.

In the Figure we see a random walk in pressure between 1 bar and 10000 bar. A random walk in potential energy is also observed and it is anti-correlated with that of pressure, as it should be.

We calculated the flucutations $\sqrt{<d^2> - <d>^2}$ of the distance d between pairs of C^α atoms. The results are shown in Fig. 6.

We see that large fluctuations are observed between residues around 7-10 and around 20-40, which are in accord with the experimental results [177, 178].

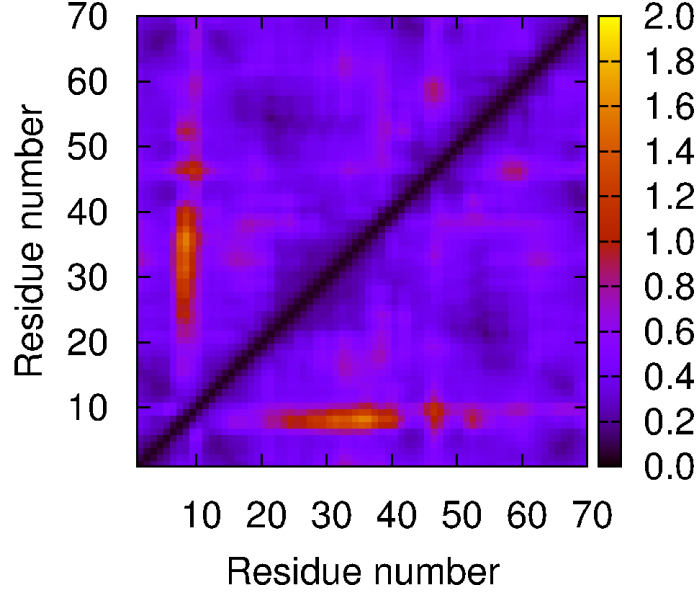The flucutating distance corresponds to that between the turn region of the β-hairpin

Figure 6: Fluctuations of distance between pairs of C^α atoms that was calculated from the PST production run.

and the end of the α-helix as depicted in Fig. 7. While at low pressure this distance is small, at high pressure it is larger and water comes into the created open region.

5   CONCLUSIONS

In this article we first introduced three well-known generalized-ensemble algorithms, namely, REM, ST, and MUCA, which can greatly enhance conformational sampling of biomolecular systems. We then presented various extensions of these algorithms. Examples are the general formulations of the multidimensional REM, ST, and MUCA. We generalized the original potential energy function E_0 by adding any physical quantities V_ℓ of interest as a new energy term with a coupling constant $\lambda^{(\ell)}(\ell = 1, \cdots, L)$. The simulations in multidimensional REM and multidimensional ST algorithms realize a random walk in temperature and $\lambda^{(\ell)}(\ell = 1, \cdots, L)$ spaces. On the other hand, the simulation in multidimensional MUCA algorithms realizes a random walk in $E_0, V_1, \cdots, V_L$ spaces.

While the multidimensional REM simulation can be easily performed because no weight factor determination is necessary, the required number of replicas can be quite large and computationally demanding. We thus prefer to use the multidimensional ST or MUCA, where only a single replica is simulated, instead of REM. However, it is very difficult to obtain optimal weight factors for the multidimensional ST and MUCA. Here, we have proposed a powerful method to determine these weight factors. Namely, we first perform a short multidimensional REM simulation and use the multiple-histogram reweighting techniques to determine the weight factors for multidimensional ST and MUCA simulations.

The multidimensional generalized-ensemble algorithms that were presented in the present article will be very useful for Monte Carlo and molecular dynamics simulations of complex systems such as spin glass, polymer, and biomolecular systems.
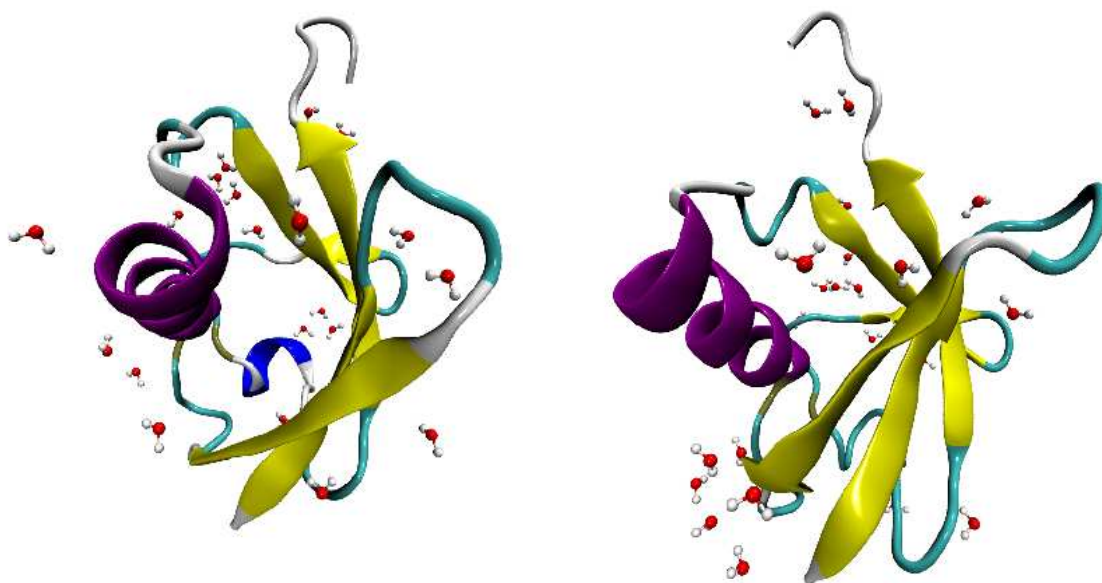
Figure 7: Snapshots of ubiquitin during the PST production run at low pressure (left) and at high pressure (right).

References

[1] Kirkpatrick, S., Gelatt, C.D. Jr., and Vecchi, M.P. (1983) Optimization by simulated annealing. *Science* **220**, 671–680.

[2] Nilges, M., Clore, G.M., and Gronenborn, A.M. (1988) Determination of three-dimensional structures of proteins from interproton distance data by hybrid distance geometry-dynamical simulated annealing calculations. *FEBS Lett.* **229**, 317–324.

[3] Brünger, A.T. (1988) Crystallographic refinement by simulated annealing. Application to a 2.8 Åresolution structure of aspartate aminotransferase. *J. Mol. Biol.* **203**, 803–816.

[4] Wilson, S.R., Cui, W., Moskowitz, J.W., and Schmidt, K.E. (1988) Conformational analysis of flexible molecules - location of the global minimum energy conformation by the simulated annealing method. *Tetrahedron Lett.* **29**, 4373–4376.

[5] Kawai, H., Kikuchi, T., and Okamoto, Y. (1989) A prediction of tertiary structures of peptide by the Monte Carlo simulated annealing method. *Protein Eng.* **3**, 85–94.

[6] Wilson, C. and Doniach, S. (1989) A computer model to dynamically simulate protein folding: studies with crambin. *Proteins* **6**, 193–209.

[7] Kawai, H., Okamoto, Y., Fukugita, M., Nakazawa, T., and Kikuchi, T. (1991) Prediction of α-helix folding of isolated C-peptide of ribonuclease A by Monte Calro simulated annealing. *Chem. Lett.* **1991**, 213–216.

[8] Okamoto, Y., Fukugita, M., Nakazawa, T., and Kawai, H. (1991) α-Helix folding by Monte Carlo simulated annealing in isolated C-peptide of ribonuclease A. *Protein Eng.* **4**, 639–647.

[9] Hansmann, U.H.E. and Okamoto, Y. (1999) Generalized-ensemble approach for protein folding simulations. In: Stauffer, D. Ed. *Annual Reviews of Computational Physics VI*, (World Scientific, Singapore) pp. 129–157.

[10] Mitsutake, A., Sugita, Y., and Okamoto, Y. (2001) Generalized-ensemble algorithms for molecular simulations of biopolymers. *Biopolymers* **60**, 96–123.

[11] Sugita, Y. and Okamoto, Y. (2002) Free-energy calculations in protein folding by generalized-ensemble algorithms. In: Schlick, T. and Gan, H.H. Eds. *Lecture Notes in Computational Science and Engineering*, (Springer-Verlag, Berlin) pp. 304–332; e-print: cond-mat/0102296.

[12] Okamoto, Y. (2004) Generalized-ensemble algorithms: enhanced sampling techniques for Monte Carlo and molecular dynamics simulations. *J. Mol. Graphics Mod.* **22**, 425–439; e-print: cond-mat/0308360.

[13] Kokubo, H. and Okamoto, Y. (2006) Replica-exchange methods and predictions of helix configurations of membrane proteins. *Mol. Sim.* **32**, 791–801.

[14] Itoh, S.G., Okumura, H., and Okamoto, Y. (2007) Generalized-ensemble algorithms for molecular dynamics simulations. *Mol. Sim.* **33**, 47–56.

[15] Sugita, Y., Mitsutake, A., and Okamoto, Y. (2008) Generalized-ensemble algorithms for protein folding simulations. In: Janke, W. Ed. *Lecture Notes in Physics. Rugged Free Energy Landscapes: Common Computational Approaches in Spin Glasses, Structural Glasses and Biological Macromolecules*, (Springer-Verlag, Berlin) pp. 369–407; e-print: arXiv:0707.3382v1[cond-mat.stat-mech].

[16] Okamoto, Y. (2009) Generalized-ensemble algorithms for studying protein folding. In: Kuwajima, K., Goto, Y., Hirata, F., Kataoka, M., and Terazima, M. Eds. *Water and Biomolecules*, (Springer-Verlag, Berlin) pp. 61–95.

[17] Ferrenberg, A.M. and Swendsen, R.H. (1988) New Monte Carlo technique for studying phase transitions. *Phys. Rev. Lett.* **61**, 2635–2638; *ibid.* **63**, 1658 (1989).

[18] Ferrenberg, A.M. and Swendsen, R.H. (1989) Optimized Monte Carlo data analysis. *Phys. Rev. Lett.* **63**, 1195–1198.

[19] Kumar, S., Bouzida, D., Swendsen, R.H., Kollman, P.A., and Rosenberg, J.M. (1992) The weighted histogram analysis method for free-energy calculations on biomolecules. 1. The method. *J. Comput. Chem.* **13**, 1011–1021.

[20] Berg, B.A. and Neuhaus, T. (1991) Multicanonical algorithms for 1st order phase transitions. *Phys. Lett.* **B267**, 249–253.

[21] Berg, B.A. and Neuhaus, T. (1992) Multicanonical ensemble: A new approach to simulate first-order phase transitions. *Phys. Rev. Lett.* **68**, 9–12.

[22] Berg, B.A. (2004) *Introduction to Monte Carlo Simulations and Their Statistical Analysis*, (World Scientific, Singapore).

[23] Janke, W. (1998) Multicanonical Monte Carlo simulations. *Physica A* **254**, 164–178.

[24] Lee, J. (1993) New Monte Carlo algorithm: Entropic sampling. *Phys. Rev. Lett.* **71**, 211–214; *ibid.* **71**, 2353 (1993).

[25] Hao, W.H. and Scheraga, H.A. (1994) Monte Carlo simulation of a first-order transition for protein folding. *J. Phys. Chem.* **98**, 4940–4948.

[26] Mezei, M. (1987) Adaptive umbrella sampling - self-consistent determination of the non-Boltzmann bias. *J. Comput. Phys.* **68**, 237–248.

[27] Bartels, C. and Karplus, M. (1998) Probability distributions for complex systems: Adaptive umbrella sampling of the potential energy. *J. Phys. Chem. B* **102**, 865–880.

[28] Torrie, G.M. and Valleau, J.P. (1977) Nonphysical sampling distributions in Monte Carlo free-energy estimation: Umbrella sampling. *J. Comput. Phys.* **23**, 187–199.

[29] Wang, F. and Landau, D.P. (2001) Efficient, multiple-range random walk algorithm to calculate the density of states. *Phys. Rev. Lett.* **86**, 2050–2053.

[30] Wang, F. and Landau, D.P. (2001) Determining the density of states for classical statistical models: a random walk algorithm to produce a flat histogram. *Phys. Rev. E* **64**, 056101.

[31] Yan, Q., Faller, R., and de Pablo, J.J. (2002) Density-of-states Monte Carlo method for simulation of fluids. *J. Chem. Phys.* **116**, 8745–8749.

[32] Laio, A. and Parrinello, M. (2002) Escaping free-energy minima. *Proc. Natl. Acad. Sci. USA* **99**, 12562–12566.

[33] Trebst, S., Huse, D.A., and Troyer, M. (2004) Optimizing the ensemble for equilibration in broad-histogram Monte Carlo simulations. *Phys. Rev. E* **70**, 046701.

[34] Berg, B.A. and Celik, T. (1992) New approach to spin-glass simulations. *Phys. Rev. Lett.* **69**, 2292–2295.

[35] Berg, B.A., Hansmann, U.H.E., and Neuhaus, T. (1993) Simulation of an ensemble with varying magnetic field: A numerical determination of the order-order interface tension in the D=2 Ising model. *Phys. Rev. B* **47**, 497–500.

[36] Janke, W. and Kappler, S. (1995) *Phys. Rev. Lett.* **74**, 212–215.

[37] Berg, B.A. and Janke, W. (1998) *Phys. Rev. Lett.* **80**, 4771–4774.

[38] Hatano, N. and Gubernatis, J.E. (2000) A multicanonical Monte Carlo study of the 3D +/- J spin glass. *Prog. Theor. Phys. (Suppl.)* **138**, 442–447.

[39] Berg, B.A., Billoire, A., and Janke, W. (2000) Spin-glass overlap barriers in three and four dimensions. *Phys. Rev. B* **61**, 12143–12150.

[40] Berg, BA., Muguruma, C., and Okamoto, Y. (2007) Residual entropy of ordinary ice from multicanonical simulations. *Phys. Rev. B* **75**, 092202.

[41] Hansmann, U.H.E. and Okamoto, Y. (1993) Prediction of peptide conformation by multicanonical algorithm - new approach to the multiple-minima problem. *J. Comput. Chem.* **14**, 1333–1338.

[42] Hansmann, U.H.E. and Okamoto, Y. (1994) Comparative study of multicanonical and simulated annealing algorithms in the protein folding problem. *Physica* **A212**, 415–437.

[43] Okamoto, Y. and Hansmann, U.H.E. (1995) Thermodynamics of helix-coil transitions studied by multicanonical algorithms. *J. Phys. Chem.* **99**, 11276–11287.

[44] Wilding, N.B. (1995) Critical-point and coexistence-curve properties of the Lennard-Jones fluid: A finite-size scaling study. *: Phys. Rev. E* **52**, 602–611.

[45] Kolinski, A., Galazka, W., and Skolnick, J. (1996) On the origin of the cooperativity of protein folding: implications from model simulations. *Proteins* **26**, 271–287.

[46] Urakami, N. and Takasu, M. (1996) Multicanonical Monte Carlo simulation of a polymer with stickers. *J. Phys. Soc. Jpn.* **65**, 2694–2699.

[47] Kumar, S., Payne, P., and Vásquez, M. (1996) Method for free-energy calculations using iterative techniques. *J. Comput. Chem.* **17**, 1269–1275.

[48] Hansmann, U.H.E., Okamoto, Y. and Eisenmenger, F. (1996) Molecular dynamics, Langevin and hybrid Monte Carlo simulations in a multicanonical ensemble. *Chem. Phys. Lett.* **259**, 321–330.

[49] Hansmann, U.H.E., and Okamoto, Y. (1996) Monte Carlo simulations in generalized ensemble: Multicanonical algorithm versus simulated tempering. *Phys. Rev. E* **54**, 5863–5865.

[50] Hansmann, U.H.E. and Okamoto, Y. (1997) Numerical comparisons of three recently proposed algorithms in the protein folding problem. *J. Comput. Chem.* **18**, 920–933.

[51] Noguchi, H. and Yoshikawa, K. (1997) First-order phase transition in a stiff polymer chain. *Chem. Phys. Lett.* **278**, 184–188.

[52] Nakajima, N., Nakamura, H., and Kidera, A. (1997) Multicanonical ensemble generated by molecular dynamics simulation for enhanced conformational sampling of peptides. *J. Phys. Chem. B* **101**, 817–824.

[53] Bartels, C. and Karplus, M. (1997) Multidimensional adaptive umbrella sampling: Applications to main chain and side chain peptide conformations. *J. Comput. Chem.* **18**, 1450–1462.

[54] Higo, J., Nakajima, N., Shirai, H., Kidera, A., and Nakamura, H. (1997) Two-component multicanonical Monte Carlo method for effective conformation sampling. *J. Comput. Chem.* **18**, 2086–2092.

[55] Iba, Y., Chikenji, G., and Kikuchi, M. (1998) Simulation of lattice polymers with multi-self-overlap ensemble. *J. Phys. Soc. Jpn.* **67**, 3327–3330.

[56] Mitsutake, A., Hansmann, U.H.E., and Okamoto, Y. (1998) Temperature dependence of distributions of conformations of a small peptide. *J. Mol. Graphics Mod.* **16**, 226–238; 262–263.

[57] Hansmann, U.H.E. and Okamoto, Y. (1999) Effects of side-chain charges on alpha-helix stability in C-peptide of ribonuclease A studied by multicanonical algorithm. *J. Phys. Chem. B* **103**, 1595–1604.

[58] Shimizu, H., Uehara, K., Yamamoto, K., and Hiwatari, Y. (1999) Structural phase transition of di-block polyampholyte. *Mol. Sim.* **22**, 285–301.

[59] Ono, S., Nakajima, N., Higo, J., and Nakamura, H. (1999) The multicanonical weighted histogram analysis method for the free-energy landscape along structural transition paths. *Chem. Phys. Lett.* **312**, 247–254.

[60] Mitsutake, A. and Okamoto, Y. (2000) Helix-coil transitions of amino-acid homo-oligomers in aqueous solution studied by multicanonical simulations. *J. Chem. Phys.* **112**, 10638–10647.

[61] Sayano, K., Kono, H., Gromiha, M.M., and Sarai, A. (2000) Multicanonical Monte Carlo calculation of the free-energy map of the base-amino acid interaction. *J. Comput. Chem.* **21**, 954–962.

[62] Yasar, F., Celik, T., Berg, B.A., and Meirovitch, H. (2000) Multicanonical procedure for continuum peptide models. *J. Comput. Chem.* **21**, 1251–1261.

[63] Mitsutake, A., Kinoshita, M., Okamoto, Y., and Hirata, F. (2000) Multicanonical algorithm combined with the RISM theory for simulating peptides in aqueous solution. *Chem. Phys. Lett.* **329**, 295–303.

[64] Cheung, M.S., Garcia, A.E., and Onuchic, J.N. (2002) Protein folding mediated by solvation: Water expulsion and formation of the hydrophobic core occur after the structural collapse. *Proc. Natl. Acad. Sci. U.S.A.* **99**, 685–690.

[65] Kamiya, N., Higo, J., and Nakamura, H. (2002) Conformational transition states of a beta-hairpin peptide between the ordered and disordered conformations in explicit water. *Protein Sci.* **11**, 2297–2307.

[66] Jang, S.M., Pak, Y., and Shin, S.M. (2002) Multicanonical ensemble with Nose-Hoover molecular dynamics simulation. *J. Chem. Phys.* **116**, 4782–4786.

[67] Terada, T., Matsuo, Y. and Kidera, A. (2003) A method for evaluating multicanonical potential function without iterative refinement: Application to conformational sampling of a globular protein in water. *J. Chem. Phys.* **118**, 4306–4311.

[68] Berg, B.A., Noguchi, H., and Okamoto, Y. (2003) Multioverlap simulations for transitions between reference configurations. *Phys. Rev. E* **68**, 036126.

[69] Bachmann, M. and Janke, W. (2003) Multicanonical chain-growth algorithm. *Phys. Rev. Lett.* **91**, 208105.

[70] Okumura, H. and Okamoto, Y. (2004) Monte Carlo simulations in multibaric-multithermal ensemble. *Chem. Phys. Lett.* **383**, 391–396.

[71] Okumura, H. and Okamoto, Y. (2004) Monte Carlo simulations in generalized isobaric-isothermal ensembles. *Phys. Rev. E* **70**, 026702.

[72] Okumura, H. and Okamoto, Y. (2004) Molecular dynamics simulations in the multibaric-multithermal ensemble. *Chem. Phys. Lett.* **391**, 248–253.

[73] Okumura, H. and Okamoto, Y. (2006) Multibaric-multithermal ensemble molecular dynamics simulations. *J. Comput. Chem.* **27**, 379–395.

[74] Itoh, S.G. and Okamoto, Y. (2004) Multi-overlap molecular dynamics methods for biomolecular systems. *Chem. Phys. Lett.* **400**, 308–313.

[75] Sugita, Y. and Okamoto, Y. (2005) Molecular mechanism for stabilizing a short helical peptide studied by generalized-ensemble simulations with explicit solvent. *Biophys. J.* **88**, 3180–3190.

[76] Itoh, S.G. and Okamoto, Y. (2007) Effective sampling in the configurational space of a small peptide by the multicanonical-multioverlap algorithm. *Phys. Rev. E* **76**, 026705.

[77] Munakata, T. and Oyama, S. (1996) Adaptation and linear-response theory. *Phys. Rev. E* **54**, 4394–4398.

[78] Lyubartsev, A.P., Martinovski, A.A., Shevkunov, S.V., and Vorontsov-Velyaminov, P.N. (1992) New approach to Monte Carlo calculation of the free energy - method of expanded ensemble. *J. Chem. Phys.* **96**, 1776–1783.

[79] Marinari, E. and Parisi, G. (1992) Simulated tempering - a new Monte Carlo scheme. *Europhys. Lett.* **19**, 451–458.

[80] Marinari, E., Parisi, G., and Ruiz-Lorenzo, J.J. (1997) Numerical simulations of spin glass systems. In: Young, A.P. Ed. *Spin Glasses and Random Fields*, (World Scientific, Singapore) pp. 59–98.

[81] Escobedo, F.A. and de Pablo, J.J. (1995) Monte Carlo simulation of the chemical potential of polymers in an expanded ensemble. *J. Chem. Phys.* **103**, 2703–2710.

[82] Irbäck, A. and Potthast, F. (1995) Studies of an off-lattice model for protein folding - sequence dependence and improved sampling at finite temperature. *J. Chem. Phys.* **103**, 10298–10305.

[83] Irbäck, A. and Sandelin, E. (1999) Monte Carlo study of the phase structure of compact polymer chains. *J. Chem. Phys.* **110**, 12256–12262.

[84] Mitsutake, A. and Okamoto, Y. (2000) Replica-exchange simulated tempering method for simulations of frustrated systems. *Chem. Phys. Lett.* **332**, 131–138.

[85] Mitsutake, A. and Okamoto, Y. (2004) Replica-exchange extensions of simulated tempering method. *J. Chem. Phys.* **121**, 2491–2504.

[86] Park, S. and Pande, V. (2007) Choosing weights for simulated tempering. *Phys. Rev. E* **76**, 016703.

[87] Zheng, L., Chen, M., and Yang, W. (2009) Simultaneous escaping of explicit and hidden free energy barriers: Application of the orthogonal space random walk strategy in generalized ensemble based conformational sampling. *J. Chem. Phys.* **130**, 234105.

[88] Zhang, C. and Ma, J. (2010) Enhanced sampling and applications in protein folding in explicit solvent. *J. Chem. Phys.* **132**, 244101.

[89] Kim, J. and Straub, J.E. (2010) Generalized simulated tempering for exploring strong phase transitions. *J. Chem. Phys.* **133**, 154101.

[90] Hukushima, K. and Nemoto, K. (1996) Exchange Monte Carlo method and application to spin glass simulations. *J. Phys. Soc. Jpn.* **65**, 1604–1608.

[91] Hukushima, K., Takayama, H., and Nemoto, K. (1996) Application of an extended ensemble method to spin glasses. *Int. J. Mod. Phys. C* **7**, 337–344.

[92] Geyer, C.J. (1991) Markov chain Monte Carlo maximum likelihood. In: Keramidas, E.M. Ed. *Computing Science and Statistics: Proc. 23rd Symp. on the Interface*, (Interface Foundation, Fairfax Station) pp. 156–163.

[93] Swendsen, R.H. and Wang, J.-S. (1986) Replica Monte Carlo simulation of spin glasses. *Phys. Rev. Lett.* **57**, 2607–2609.

[94] Kimura, K. and Taki, K. (1991) Time-homogeneous parallel annealing algorithm. Vichnevetsky, R. and J.J.H. Miller, J.J.H. Eds. In: *Proc. 13th IMACS World Cong. on Computation and Appl. Math. (IMACS '91)*, vol. 2, pp. 827–828.

[95] Frantz, D.D., Freeman, D.L., and Doll, J.D. (1990) Reducing quasi-ergodic behavior in Monte Carlo simulations by J-walking - applications to atomic clusters. *J. Chem. Phys.* **93**, 2769–2784.

[96] Tesi, M.C., van Rensburg, E.J.J., Orlandini, E., and Whittington, S.G. (1996) Monte Carlo study of the interacting self-avoiding walk model in three dimensions. *J. Stat. Phys.* **82**, 155–181.

[97] Iba, Y. (2001) Extended ensemble Monte Carlo. *Int. J. Mod. Phys. C* **12**, 623–656.

[98] Hansmann, U.H.E. (1997) Parallel tempering algorithm for conformational studies of biological molecules. *Chem. Phys. Lett.* **281**, 140–150.

[99] Sugita, Y. and Okamoto, Y. (1999) Replica-exchange molecular dynamics method for protein folding. *Chem. Phys. Lett.* **314**, 141–151.

[100] Wu, M.G. and Deem, M.W. (1999) Efficient Monte Carlo methods for cyclic peptides. *Mol. Phys.* **97**, 559–580.

[101] Sugita, Y., Kitao, A., and Okamoto, Y. (2000) Multidimensional replica-exchange method for free-energy calculations. *J. Chem. Phys.* **113**, 6042–6051.

[102] Woods, C.J., Essex, J.W., and King, M.A. (2003) The development of replica-exchange-based free-energy methods. *J. Phys. Chem. B* **107**, 13703–13710.

[103] Sugita, Y. and Okamoto, Y. (2000) Replica-exchange multicanonical algorithm and multicanonical replica-exchange method for simulating systems with rough energy landscape. *Chem. Phys. Lett.* **329**, 261–270.

[104] Gront, D., Kolinski, A., and Skolnick, J. (2000) Comparison of three Monte Carlo conformational search strategies for a proteinlike homopolymer model: Folding thermodynamics and identification of low-energy structures. *J. Chem. Phys.* **113**, 5065–5071.

[105] Verkhivker, G.M., Rejto, P.A., Bouzida, D., Arthurs, S.,Colson, A.B., Freer, S.T., Gehlhaar, D.K., Larson, V., Luty, B.A., Marrone, T., and Rose, P.W. (2001) Parallel simulated tempering dynamics of ligand-protein binding with ensembles of protein conformations. *Chem. Phys. Lett.* **337**, 181–189.

[106] Fukunishi, F., Watanabe, O., and Takada, S. (2002) On the Hamiltonian replica exchange method for efficient sampling of biomolecular systems: Application to protein structure prediction. *J. Chem. Phys.* **116**, 9058–9067.

[107] Mitsutake, A., Sugita, Y., and Okamoto, Y. (2003) Replica-exchange multicanonical and multicanonical replica-exchange Monte Carlo simulations of peptides. I. Formulation and benchmark test. *J. Chem. Phys.* **118**, 6664–6675.

[108] Mitsutake, A., Sugita, Y., and Okamoto, Y. (2003) Replica-exchange multicanonical and multicanonical replica-exchange Monte Carlo simulations of peptides. II. Application to a more complex system. *J. Chem. Phys.* **118**, 6676–6688.

[109] Sikorski, A. and Romiszowski, P. (2003) Thermodynamical properties of simple models of protein-like heteropolymers. *Biopolymers* **69**, 391–398.

[110] Lin, C.Y., Hu, C.K., and Hansmann, U.H.E. (2003) Parallel tempering simulations of HP-36. *Proteins* **52**, 436–445.

[111] La Penna, G., Mitsutake, A., Masuya, M., and Okamoto, Y. (2003) Molecular dynamics of C-peptide of ribonuclease A studied by replica-exchange Monte Carlo method and diffusion theory. *Chem. Phys. Lett.* **380**, 609–619.

[112] Kokubo, H. and Okamoto, Y. (2004) Prediction of membrane protein structures by replica-exchange Monte Carlo simulations: Case of two helices. *J. Chem. Phys.* **120**, 10837.

[113] Kokubo, H. and Okamoto, Y. (2009) Analysis of helix-helix interactions of bacteriorhodopsin by replica-exhcange simulations. *Biophys. J.* **96**, 765–776.

[114] Falcioni, M. and Deem, D.W. (1999) A biased Monte Carlo scheme for zeolite structure solution. *J. Chem. Phys.* **110**, 1754–1766.

[115] Yan, Q. and de Pablo, J.J. (1999) Hyper-parallel tempering Monte Carlo: Application to the Lennard-Jones fluid and the restricted primitive model. *J. Chem. Phys.* **111**, 9509–9516.

[116] Nishikawa, T., Ohtsuka, H., Sugita, Y., Mikami, M., and Okamoto, Y. (2000) Replica-exchange Monte Carlo method for Ar fluid. *Prog. Theor. Phys. (Suppl.)* **138**, 270–271.

[117] Kofke, D.A. (2002) On the acceptance probability of replica-exchange Monte Carlo trials. *J. Chem. Phys.* **117**, 6911–6914.

[118] Okabe, T., Kawata, M., Okamoto, Y., and Mikami, M. (2001) Replica-exchange Monte Carlo method for the isobaric-isothermal ensemble. *Chem. Phys. Lett.* **335**, 435–439.

[119] Ishikawa, Y., Sugita, Y., Nishikawa, T., and Okamoto, Y. (2001) Ab initio replica-exchange Monte Carlo method for cluster studies. *Chem. Phys. Lett.* **333**, 199–206.

[120] Garcia, A.E. and Sanbonmatsu, K.Y. (2001) Exploring the energy landscape of a beta hairpin in explicit solvent. *Proteins* **42**, 345–354.

[121] Zhou, R.H., Berne, B.J., and Germain, R. (2001) The free energy landscape for beta hairpin folding in explicit water. *Proc. Natl. Acad. Sci. U.S.A.* **98**, 14931–14936.

[122] Garcia, A.E. and Sanbonmatsu, K.Y. (2002) α-Helical stabilization by side chain shielding of backbone hydrogen bonds. *Proc. Natl. Acad. Sci. U.S.A.* **99**, 2782–2787.

[123] Zhou, R.H. and Berne, B.J. (2002) *Proc. Natl. Acad. Sci. U.S.A.* **99**, 12777–12782.

[124] Feig, M. MacKerell, A.D., and Brooks, C.L. III (2003) Force field influence on the observation of pi-helical protein structures in molecular dynamics simulations. *J. Phys. Chem. B* **107**, 2831–2836.

[125] Rhee, Y.M. and Pande, V.S. (2003) Multiplexed-replica exchange molecular dynamics method for protein folding simulation. *Biophys. J.* **84**, 775–786.

[126] Paschek, D. and Garcia, A.E. (2004) Reversible temperature and pressure denaturation of a protein fragment: A replica exchange molecular dynamics simulation study. *Phys. Rev. Lett.* **93**, 238105.

[127] Paschek, D., Gnanakaran, S., and Garcia, A.E. (2005) Simulations of the pressure and temperature unfolding of an α-helical peptide. *Proc. Natl. Acad. Sci. USA* **102**, 6765–6770.

[128] Pitera, J.W. and Swope, W. (2003) Understanding folding and design: Replica-exchange simulations of "Trp-cage" fly miniproteins. *Proc. Natl. Acad. Sci. U.S.A.* **100**, 7587–7592.

[129] Ohkubo, Y.Z. and Brooks, C.L. III (2003) Exploring Flory's isolated-pair hypothesis: Statistical mechanics of helix-coil transitions in polyalanine and the C-peptide from RNase A. *Proc. Natl. Acad. Sci. U.S.A.* **100**, 13916–13921.

[130] Fenwick, M.K. and Escobedo, F.A. (2003) Hybrid Monte Carlo with multidimensional replica exchanges: Conformational equilibria of the hypervariable reigons of a llamma V-HH antibody domain. *Biopolymers* **68**, 160–177.

[131] Xu, H.F. and Berne, B.J. (2000) Multicanonical jump walking annealing: an efficient method for geometric optimization. *J. Chem. Phys.* **112**, 2701–2708.

[132] Faller, R., Yan, Q., and de Pablo, J.J. (2002) Multicanonical parallel tempering. *J. Chem. Phys.* **116**, 5419–5423.

[133] Fenwick, M.K. and Escobedo, F.A. (2003) Expanded ensemble and replica exchange methods for simulation of protein-like systems. *J. Chem. Phys.* **119**, 11998–12010.

[134] Murata, K., Sugita, Y., and Okamoto, Y. (2004) Free energy calculations for DNA base stacking by replica-exchange umbrella sampling. *Chem. Phys. Lett.* **385**, 1–7.

[135] Felts, A.K., Harano, Y., Gallicchio, E., and Levy, R.M. (2004) Free energy surfaces of β-hairpin and α-helical peptides generated by replica exchange molecular dynamics with the AGBNP implicit solvent model. *Proteins* **56**, 310–321.

[136] Mitsutake, A., Kinoshita, M., Okamoto, Y., and Hirata, F. (2004) Combination of the replica-exchange Monte Carlo method and the reference interaction site model theory for simulating a peptide molecule in aqueous solution. *J. Phys. Chem. B* **108**, 19002–19012.

[137] Baumketner, A. and Shea, J.E. (2005) Free energy landscapes for amyloidogenic tetrapeptides dimerization. *Biophys. J.* **89**, 1493–1503.

[138] Yoda, T., Sugita, Y., and Okamoto, Y. (2007) Cooperative folding mechanism of a beta-hairpin peptide studied by a multicanonical replica-exchange molecular dynamics simulation. *Proteins* **66**, 846–859.

[139] Roitberg, A.E., Okur, A., and Simmerling, C. (2007) Coupling of replica exchange simulations to a non-Boltzmann structure reservoir. *J. Phys. Chem. B* **111**, 2415–2418.

[140] Rosta, E., Buchete, N.-Y., and Hummber, G. (2009) Thermostat artifacts in replica exchange molecular dynamics simulations. *J. Chem. Theory Comput.* **5**, 1393–1399.

[141] Yoda, T., Sugita, Y., and Okamoto, Y. (2010) Hydrophobic core formation and dehydration in protein folding studied by generalized-ensemble simulaitons. *Biophys. J.* **99**, 1637–1644.

[142] De Simone, A. and Derreumaux, P. (2010) Low molecular weight oligomers of amyloid peptides display β-barrel conformations: A replica exchange molecular dynamics study in explicit solvent. *J. Chem. Phys.* **132**, 165103.

[143] Hukushima, K. (1999) Domain-wall free energy of spin-glass models: Numerical method and boundary conditions. *Phys. Rev. E* **60**, 3606–3614.

[144] Whitfield, T.W., Bu, L., and Straub, J.E. (2002) Generalized parallel sampling. *Physica A* **305**, 157–171.

[145] Kwak, W. and Hansmann, U.H.E. (2005) Efficient sampling of protein structures by model hopping. *Phys. Rev. Lett.* **95**, 138102.

[146] Bunker, A. and Dünweg, B. (2000) Parallel excluded volume tempering for polymer melts. *Phys. Rev. E* **63**, 016701.

[147] Liu, P., Kim, B., Friesner, R.A., and Bern, B.J. (2005) Replica exchange with solute tempering: A method for sampling biological systems in explicit water. *Proc. Natl. Acad. Sci. U.S.A.* **102**, 13749–13754.

[148] Affentranger, R., Tavernelli, I., and Di Iorio, E.E. (2006) A novel Hamiltonian replica exchange MD protocol to enhance protein conformational space sampling. *J. Chem. Theory Comput.* **2**, 217–228.

[149] Lou, H. and Cukier, R.I. (2006) Molecular dynamics of apo-adenylate kinase: A distance replica exchange method for the free energy of conformational fluctuations. *J. Phys. Chem. B* **110**, 24121–24137.

[150] Mu, Y. (2009) Dissociation aided and side chain sampling enhanced Hamiltonian replica exchange. *J. Chem. Phys.* **130**, 164107.

[151] Itoh, S.G., Okumura, H., and Okamoto, Y. (2010) Replica-exchange method in van der Waals radius space: Overcoming steric restrictions for biomolecules. *J. Chem. Phys.* **132**, 134105.

[152] Mitsutake, A. and Okamoto, Y. (2009) From multidimensional replica-exchange method to multidimensional multicanonical algorithm and simulated tempering. *Phys. Rev. E* **79**, 047701.

[153] Mitsutake, A. and Okamoto, Y. (2009) Multidimensional generalized-ensemble algorithms for complex systems. *J. Chem. Phys.* **130**, 214105.

[154] Mitsutake, A. (2009) Simulated-tempering replica-exchange method for the multidimensional version. *J. Chem. Phys.* **131**, 094105.

[155] Mori, Y. and Okamoto, Y. (2010) Generalized-ensemble algorithms for the isobaric-isothermal ensemble. *J. Phys. Soc. Jpn.* **79**, 074003.

[156] N. Metropolis, N., A.W. Rosenbluth, A.W., M.N. Rosenbluth, M.N., A.H. Teller, A.H., and E. Teller, E. (1953) Equation of state calculations by fast computing machines. *J. Chem. Phys.* **21**, 1087–1092.

[157] Nosé, S. (1984) A molecular dynamics method for simulations in the canonical ensemble. *Mol. Phys.* **52**, 255–268.

[158] Nosé, S. (1984) A unified formulation of the constant temperature molecular dynamics methods. *J. Chem. Phys.* **81**, 511–519.

[159] Shirts, M.R. and Chodera, J.D. (2008) Statistically optimal analysis of samples from multiple equilibrium states. *J. Chem. Phys.* **129**, 124105.

[160] Berg, B.A. (2003) Multicanonical simulations step by step. *Comp. Phys. Commun.* **153**, 397–406.

[161] Mori, Y. and Okamoto, Y. (2010) Replica-exchange molecular dynamics simulations for various constant temperature algorithms. *J. Phys. Soc. Jpn.* **79**, 074001.

[162] Allen, M.P. and Tildesley, D.J. (1987) *Computer Simulation of Liquids* (Oxford, New York) p. 259.

[163] Andersen, H.G. (1980) Molecular dynamics simulations at constant pressure and/or temperature. *J. Chem. Phys.* **72**, 2384–2393.

[164] Hoover, W.G., Ladd, A.J.C., and Moran, B. (1982) High strain rate plastic flow studied via non-equilibrium molecular dynamics. *Phys. Rev. Lett.* **48**, 1818–1820.

[165] Evans, D.J. (1983) Computer experiment for non-linear thermodynamics of couette flow. *J. Chem. Phys.* **78**, 3297–3302.

[166] Evans, D.J. and Morriss, G.P. (1983) The isothermal isobaric molecular dynamics ensemble. *Phys. Lett. A* **98**, 433–436.

[167] Hoover, W.G. (1985) Canonical dynamics - equilibrium phase space distributions. *Phys. Rev. A* **31**, 1695–1697.

[168] Martyna, G.J., Klein, M.L., and Tuckerman, M. (1992) Nosé-Hoover chains - the canonical ensemble via continuous dynamics. *J. Chem. Phys.* **97**, 2635–2643.

[169] Bond, S.D., Leimkuhler, B.J., and Laird, B.B. (1999) The Nosé-Poincaré method for constant temperature molecular dynamics. *J. Comput. Phys.* **151**, 114–134.

[170] McDonald, I.R. (1972) NpT-ensemble Monte Carlo calculations for binary liquid mixtures. *Mol. Phys.* **23**, 41-58.

[171] Myers, J.K., Pace, C.N., and Scholtz, J.M. (1997) A direct comparison of helix propensity in proteins and peptides. *Proc. Natl. Acad. Sci. U.S.A.* **94**, 2833–2837.

[172] Momany, F.A., McGuire, R.F., Burgess, A.W., and Scheraga, H.A. (1975) Energy parameters in polypeptides. VII. Geometric parameters, partial atomic charges, nonbonded interactions, hydrogen bond interactions, and intrinsic torsional potentials for the naturally occurring amino acids. *J. Phys. Chem.* **79**, 2361–2381.

[173] Némethy, G., Pottle, M.S., and Scheraga, H.A. (1983) Energy parameters in polypeptides. 9. Updating of geometrical parameters, nonbonded interactions, and hydrogen bond interactions for the naturally occurring amino acids. *J. Phys. Chem.* **87**, 1883–1887.

[174] Sippl, M.J., Némethy, G., and Scheraga, H.A. (1984) Intermolecular potentials from crystal data. 6. Determination of empirical potentials for O-H...O=C hydrogen bonds from packing configurations. *J. Phys. Chem.* **88**, 6231–6233.

[175] Ooi, T., Oobatake, M., Némethy, G., and Scheraga, H.A. (1987) Accessible surface areas as a measure of the thermodynamic parameters of hydration of peptides. *Proc. Natl. Acad. Sci. U.S.A.* **84**, 3086–3090.

[176] Masuya, M., unpublished; see http://biocomputing.cc/nsol/.

[177] Kitahara, R. and Akasaka, K. (2003) Close identity of a pressure-stabilized intermediate with a kinetic intermediate in protein folding. *Proc. Natl. Acad. Sci. U.S.A.* **100**, 3167–3172.

[178] Kitahara, R., Yokoyama, S., and Akasaka, K. (2005) NMR snapshots of a fluctuating protein structure: ubiquitin at 30 bar - 3 kbar. *J. Mol. Biol.* **347**, 277–285.

[179] Quigley, D. and Probert, M.I.J. (2004) Landevin dynamics in constant pressure extended systems. *J. Chem. Phys.* **120**, 11432–11441.

[180] Darden, T., York, D., and Pedersen, L. (1993) Particle mesh Ewald - an Nlog(N) method for Ewald sums in large systems. *J. Chem. Phys.* **98**, 10089–10092.

[181] Essmann, U., Perera, L., Berkowitz, M.L., Darden, T., Lee, H., and Pedersen, L.G. (1995) A smooth particle mesh Ewald method. *J. Chem. Phys.* **103**, 8577–8593.

[182] MacKerell, A.D. Jr., Bashford, D., Bellott, M., Dunbrack, R.L. Jr., Evanseck, J.D., Field, M.J., Fischer, S., Gao, J., Guo, H., Ha, S., Joseph-McCarthy, D., Kuchnir, L., Kuczera, K., Lau, F.T.K., Mattos, C., Michnick, S., Ngo, T., Nguyen, D.T., Prodhom, B., Reiher, W.E. III, Roux, B., Schlenkrich, M., Smith, J.C., Stote, R., Straub, J., Watanabe, M., Wiórkiewicz-Kuczera, J., Yin, D., and Karplus, M. (1998) All-atom empirical potential for molecular modeling and dynamics studies of proteins. *J. Phys. Chem. B* **102**, 3586–3616.

[183] MacKerell, A.D. Jr., Feig, M., and Brooks, C.L. III (2004) Improved treatment of the protein backbone in empirical force fields. *J. Am. Chem. Soc.* **126**, 698–699.

[184] MacKerell, A.D. Jr., Feig, M., and Brooks, C.L. III (2004) Extending the treatment of backbone energetics in protein force fields: Limitations of gas-phase quantum mechanics in reproducing protein conformational distributions in molecular dynamics simulations. *J. Comput. Chem.* **25**, 1400–1415.

[185] Jorgensen, W.L., Chandrasekhar, J., Madura, J.D., Impey, R.W., Klein, M.L. (1983) Comparison of simple potential functions for simulating liquid water. *J. Chem. Phys.* **79**, 926–935.

[186] Phillips, J.C., Braun, R., Wang, W., Gumbart, J., Tajkhorshid, E., Villa, E., Chipot, C., Skeel, R.D., Kale, L., and Schulten, K. (2005) Scalable molecular dynamics with NAMD. *J. Comput. Chem.* **26**, 1781–1802.